



A Concept for Preoperative and Intraoperative Molecular Imaging and Detection for Assessing Extent of Disease of Solid Tumors

Charles L. Hitchcock^{1,2*}, Gregg J. Chapman^{2,3}, Cathy M. Mojzisek², Jerry K. Mueller Jr.² and Edward W. Martin Jr.^{2,4}

¹Department of Pathology, College of Medicine, The Ohio State University, Columbus, OH, United States, ²Actis Medical, LLC, Powell, OH, United States, ³Department of Electrical and Computer Engineering, College of Engineering, The Ohio State University, Columbus, OH, United States, ⁴Division of Surgical Oncology, Department of Surgery, College of Medicine, The Ohio State University, Columbus, OH, United States

The authors propose a concept of “systems engineering,” the approach to assessing the extent of diseased tissue (EODT) in solid tumors. We modeled the proof of this concept based on our clinical experience with colorectal carcinoma (CRC) and gastrinoma that included short and long-term survival data of CRC patients. This concept, applicable to various solid tumors, combines resources from surgery, nuclear medicine, radiology, pathology, and oncology needed for preoperative and intraoperative assessments of a patient’s EODT. The concept begins with a patient presenting with biopsy-proven cancer. An appropriate preferential locator (PL) is a molecule that preferentially binds to a cancer-related molecular target (i.e., tumor marker) lacking in non-malignant tissue and is the essential element. Detecting the PL after an intravenous injection requires the PL labeling with an appropriate tracer radionuclide, a fluoroprobe, or both. Preoperative imaging of the tracer’s signal requires molecular imaging modalities alone or in combination with computerized tomography (CT). These include positron emission tomography (PET), PET/CT, single-photon emission computed tomography (SPECT), SPECT/CT for preoperative imaging, gamma cameras for intraoperative imaging, and gamma-detecting probes for precise localization. Similarly, fluorescent-labeled PLs require appropriate cameras and probes. This approach provides the surgeon with real-time information needed for R0 resection.

OPEN ACCESS

Edited by:

Mauro Cives,
University of Bari Aldo Moro, Italy

Reviewed by:

Javier Retamales,
Grupo Oncológico Cooperativo
Chileno de Investigación, Chile
Angela Cappello,
University of Bari Aldo Moro, Italy

*Correspondence:

Charles L. Hitchcock,
✉ emerituschuck@gmail.com

Received: 30 March 2024

Accepted: 28 May 2024

Published: 25 July 2024

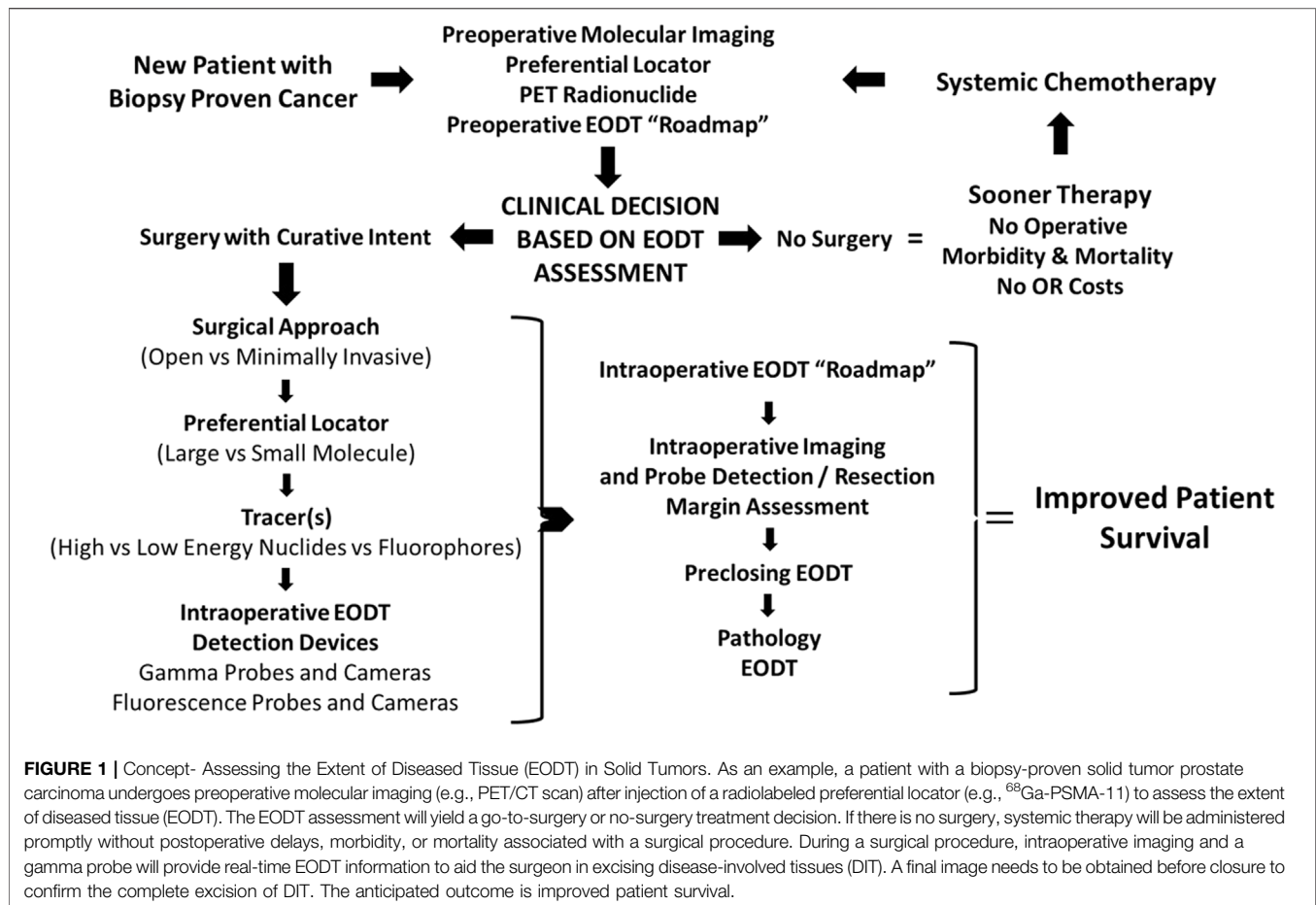
Citation:

Hitchcock CL, Chapman GJ,
Mojzisek CM, Mueller JK Jr.,
Martin EW Jr. (2024) A Concept for
Preoperative and Intraoperative
Molecular Imaging and Detection for
Assessing Extent of Disease of
Solid Tumors.
Oncol. Rev. 18:1409410.
doi: 10.3389/or.2024.1409410

Keywords: radionuclide, fluorescence, guided-surgery, intraoperative-imaging, fluorescence-guided surgery

INTRODUCTION

Surgery remains the primary curative treatment for colorectal carcinoma (CRC) and other solid tumors. Hall and Ruutinen [1] stated that in the case of CRC, “complete excision of all areas of disease provides the only curative treatment of all stages of localized disease (stages I-III), and stage IV disease with limited liver and lung metastases.” This article goes beyond routine pathology findings. We refer to “disease-involved tissue” (DIT) as tissue that may or may not contain apparent metastatic tumor cells on routine histopathologic examination; however, this tissue binds the PL, which is demonstrated on molecular imaging or probing, thus indicating disease involvement. Our



experience demonstrates that incomplete identification of DIT leads to clinical decisions that can result in unresected disease, a significant cause of morbidity and mortality [2, 3]. The tissue left behind after cytoreductive surgery may be immunocompromised. In the case of CRC, recurrence usually occurs within 2 years of primary surgery, and distant recurrence sites vary between colon and rectal tumors. In contrast, local recurrences occur at the margins and in unresected lymph nodes associated with aberrant lymphatics and lymph nodes outside the anatomic planes of resection [3–5]. An accurate, real-time EODT assessment will optimize intraoperative treatment decisions, thereby reducing the incidence of recurrence while improving patient survival.

HYPOTHESIS AND THEORY: PROOF OF CONCEPT

The Concept

Using our experience with colorectal carcinoma and, more recently, neuroendocrine carcinomas at The Ohio State University Wexner Medical Center over the past four decades, the authors propose a “systems engineering” concept for assessing the EODT in solid tumors. **Figure 1** depicts a model for this concept. This model, applicable to various solid tumors,

combines resources from surgery, nuclear medicine, radiology, pathology, and oncology needed for preoperative and intraoperative assessments of a patient’s EODT. The model begins with a patient presenting to the team with biopsy-proven cancer. The concept’s essential element is a preferential locator (PL), a targeting molecule that preferentially binds to specific tumor-associated molecules not expressed in non-malignant tissues. PL detection requires labeling with an appropriate tracer radionuclide, a fluoroprobe, or both. Preoperative imaging and intraoperative imaging and detection of a radionuclide tracer’s signal utilize a wide variety of modalities (e.g., PET, PET/CT, SPECT, SPECT/CT, portable gamma cameras, and gamma-detecting probes), and fluorescent cameras and probes use fluorochrome-labeled PLs. However, the inherent variability of each imaging and detection technique is still present. In addition, the concept addresses the impact on the patient when a “No Surgery” clinical decision is made. The “No Surgery” decision allows the patient to undergo medical therapy immediately without treatment delays relative to postoperative recovery and eliminates any morbidity and mortality associated with a non-curative surgery. The “no surgery” clinical decision is not a final one. Molecular reimaging to assess for the EODT should be a critical part of the follow-up for patients receiving systemic neoadjuvant

chemotherapy in order to balance “the need for radical removal of disease and minimizing the scope of surgery.” [6]

Initial EODT assessment requires preoperative hybrid molecular imaging (e.g., PET/CT or SPECT/CT) to provide a “roadmap” of the locations of the DIT that correlates both the anatomic and molecular features of the tumor. However, this correlation depends on the PL the multidisciplinary team members selected [7, 8]. Using the EODT “roadmap,” the surgeon decides whether surgery is the best option for managing the primary disease and with an oncologist for managing recurrent disease. The key here is that the right tools are selected to meet the individual needs of the patient’s case. If surgery is a “no-go,” the multidisciplinary team decides the best treatment options, as are the nature and timing of follow-up assessments. The decision to use an open or minimally invasive approach for surgery with curative intent determines the surgeon’s plan for obtaining the “intraoperative real-time assessment of EODT.” Again, a series of decisions must be made, including 1), if needed, which preferential locator to use; 2) what type of tracer, radionuclide vs. fluoroprobe, should label the PL; and 3) which intraoperative imaging cameras and detection probes to use. Real-time EODT assessment with concurrent use of an intraoperative gamma camera and detection probe allows the surgeon to image the surgical field, precisely excise DIT, and reimage the field before closure of the abdomen to ensure no unresected DIT remains, especially at the margins.

EODT for pathology may involve imaging the resected surgical specimen(s) and marking the site of DIT in the specimen before sending it to surgical pathology [9]. This approach correlates the pathologic assessment with the surgical findings, enhancing accurate staging and subsequent treatment decision-making. Does this “systems engineering” approach to surgical oncology work? We have successfully used this approach in patients with gastrinoma [10] and others with different solid tumors [6, 10, 11]. (See **Figure 6** below.).

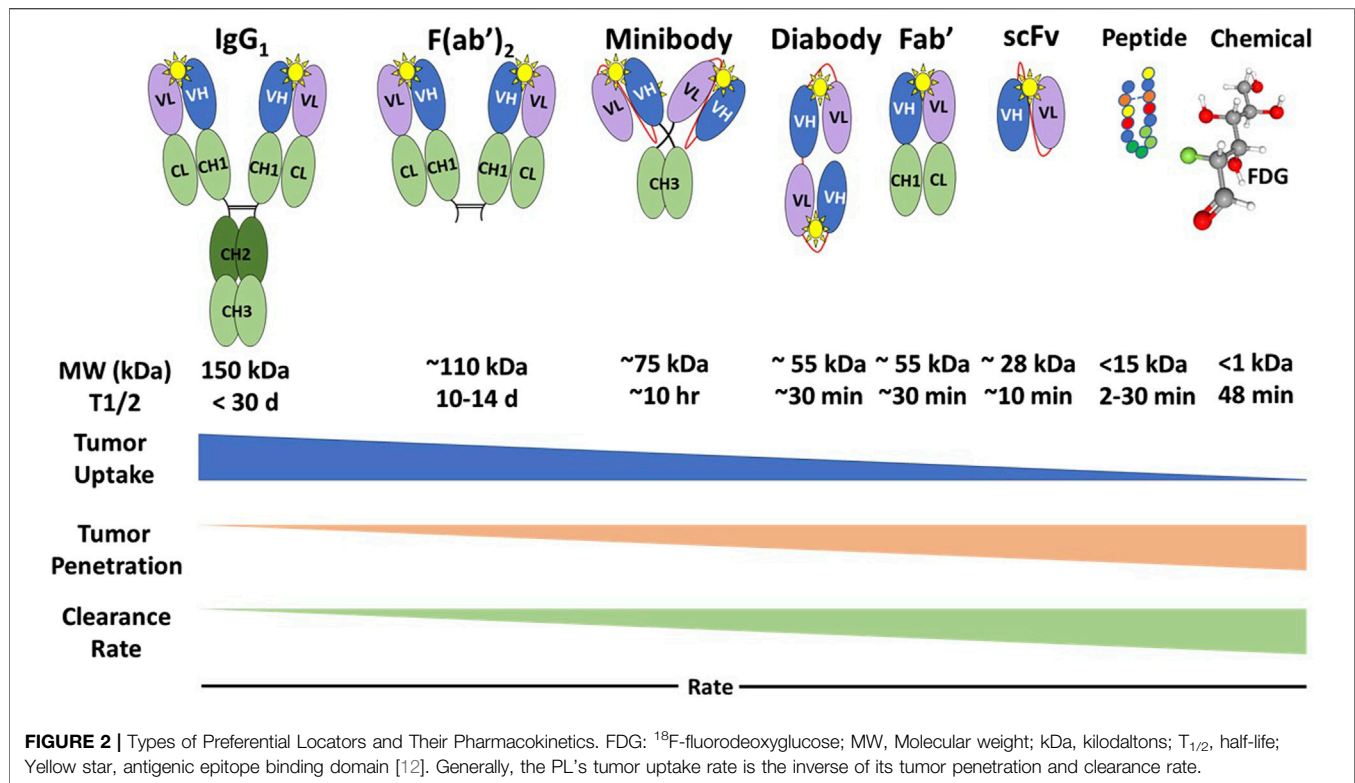
Colorectal Carcinoma as an Exemplar the Concept of EODT Assessment

Three different imaging modalities—*anatomic, functional, or hybrid anatomic/functional*—provide preoperative images. Based on morphologic imaging, current preoperative imaging techniques do not accurately map the EODT for CRC [15]. The National Comprehensive Cancer Network (NCCN) guidelines call for preoperative imaging using CT scans, with contrast, of the chest, abdomen, and pelvis [16]. Similarly, the American College of Radiology (ACR) recommendations include chest CT and magnetic resonance imaging (MRI) to assess rectal and colon cancer [17]. MRI is more commonly used to assess hepatic metastases and for staging rectal cancer. Variations in instrumentation, protocols, and level of experience of the reader play a critical role in the ability of CT and MRI imaging to recognize DIT, with a reported accuracy of approximately 70% for mapping lymph node metastases [18–20]. This problem is exemplified by Olsen and others [21], who found the inaccurate staging of 35% of primary CRC cases in their retrospective study of 3465 Danish

patients, which included 36% of patients with regional metastases and 58% of patients with clinical stage I disease. Similarly, Reali et al. [22] reported in their study that preoperative staging in 948 CRC patients found correct T and N staging in only 19.68% of colon cancer patients compared to 53.85% of patients with rectal cancer. These discordant results, in part, are due to CT and MRI detection of lymph nodes, either benign or metastatic, are limited to those nodes 5 mm or larger and by the reproducibility of morphologic criteria [23]. However, metastases often occur in mesenteric lymph nodes below this 5 mm size detection level [24–27]. In a study of 6969 lymph nodes from CRC patients, Schrembs et al. [28] reported that the majority of lymph nodes identified fell between 1 and 6 mm in diameter, with 39% 3 mm or less in diameter, and 5.24 mm being the median size of positive lymph nodes as compared to 4.14 mm for negative lymph nodes. Current machine learning tools developed to improve this accuracy lack standardization in instrumentation, sample size, and algorithms needed to predict which preoperative CRC patients lack lymph node metastases [29, 30].

Unlike the anatomic information provided by CT and MRI imaging, molecular imaging provides functional information at the cellular and molecular levels. Molecular imaging requires a PL, a molecule (e.g., binding to a tumor-specific biomarker (e.g., protein, receptor) labeled with a radionuclide tracer. The tracer’s decay gives rise to photons imaged by SPECT or PET. Hybrid imaging, a combination of CT or MRI with either SPECT or PET, provides higher-resolution images than PET or SPECT alone. The image quality and spatial resolution of PET and PET/CT are improved. However, there are only a few clinical applications for SPECT and SPECT/CT in the preoperative imaging of solid tumors [31]. As evidenced by the recent Food and Drug Administration (FDA) approval of several new PET-based radiopharmaceuticals for neuroendocrine [32] and prostate carcinomas [33, 34], there is an increasing acceptance of molecular imaging in assessing EODT of solid tumors. Molecular imaging has led to many preclinical and early clinical studies of various biomarkers as possible targets for imaging in CRC and other cancers [35–39].

Armed with the preoperative image-derived roadmap, the surgeon must decide on the surgical approach. The success of a curative surgical procedure requires resection of all DIT. Based on an open surgical approach, our data indicates that if all gamma-positive tissue, regardless of pathology findings and staging, is removed, there is a significant overall survival advantage for patients with primary or recurrent CRC at 5 years or greater [40–42]. Most cases involved direct supervision by a select academic faculty specializing in surgical oncology or colorectal surgery. Today, minimally invasive surgery (MIS), either laparoscopic or robotic, is replacing the open procedure. MIS provides patients with a shorter hospital stay, reduced postoperative pain, improved bowel function return, reduced incidence of wound infections, and improved cosmesis [43]. The variability among surgeons’ technical experience with various open and minimally invasive procedures is well known [44, 45]. With MIS, the surgeon’s visual and tactile senses are often reduced. A potential



drawback of laparoscopy is the inability to predict which patients require conversion to open surgery. Robotics reduce the problems of 2D visualization, maneuverability, and tremors by providing a stable camera, 3D magnification, and wrist-like dexterity. However, it comes at a much higher cost, longer operating room time, and reduced haptic control [46, 47]. The proposed EODT assessment approach will help reduce the learning curve and better predict patients with an open surgical procedure associated with MIS while adding auditory and visual information in real time regarding the extent and location of DIT. The surgical procedure will influence the subsequent selection of preferential locators, tracer labeling, and methods for detecting the tracer signal, especially in fluorescence-guided surgery cases.

Examples of Preferential Locators

Cancer cells overexpress many biomarkers that are targets for PL in assessing EODT. However, there is no single cancer-specific target molecule. The ideal biomarker for PLs includes cellular and acellular components within the tumor's extracellular matrix and molecules on the cell membranes of tumor cells. The latter includes overexpressed membrane glycoconjugates, proteins, receptors, transporters, and enzymes. In addition, intracellular molecules involved in altered cellular metabolic processes, e.g., cell proliferation or glucose metabolism, can serve as targets for PLs. It is important to note that the expression of these target molecules is heterogeneous among tumors, within a given tumor, among tumor cells, and between the primary and metastatic foci.

Regardless of the type of molecules, PLs for EODT assessment must exhibit high affinity (i.e., the ability for initial binding to the target molecule) and high avidity (i.e., the ability to remain bound to the target molecule over time) that allows the rapid clearance needed for a high tumor-to-background ratio (TBR) that optimizes imaging and detection of DIT. A PL's molecular features—structure, size, mass, and charge—determine its pharmacokinetics and potential clinical applications (Figure 2).

The intact IgG monoclonal antibody (MoAb) has two identical heavy chains that contain a variable domain (VH) and three constant domains (CH1, CH2, and CH3), and two identical light chains containing a variable domain (VL) and a constant domain (CL). The IgG has two antigenic epitope binding domains (Figure 2, yellow star) formed by the two variable domains (VL and VH). Intact MoAbs have a slow plasma clearance, resulting in a 2-3-week half-life. Murine MoAbs (mMoAb) can induce unwanted human anti-mouse antibodies (HAMA) that can alter imaging results. Bioengineering of a chimeric MoAb with a murine or a human variable region and human constant regions minimizes immunogenicity while maintaining the affinity and avidity of the MoAb. The slow clearance allows for tumor uptake, penetration, and accumulation of the intact mMoAb but requires labeling with a radionuclide with a long half-life. This delay provides time for multiple imaging studies and optimization of surgical planning and intraoperative EODT assessment [46]. However, MoAb size requires hepatic rather than renal clearance, which may preclude the detection of liver metastases. In addition, the slow clearance and nonspecific

TABLE 1 | FDA-Approved Preferential Locators for Molecular Imaging and Fluorescence-Guided Surgery. * No longer marketed in the U.S.; FDG: ^{18}F -fluorodeoxyglucose; DCFPyI: 2-(3-(1-carboxy-5-[(6- ^{18}F -fluoro-pyridine-3-carbonyl)-amino]-pentyl)-ureido)-pentanedioic acid; PSMA: prostate specific membrane antigen; NET: neuroendocrine carcinoma; TAG-72: tumor associated glycoprotein-72; NIR: near infrared; FGS: fluorescence guided surgery.

Preferential locator (FDA approval Date)	Product Name	Tumor	Target	Tracer	Application
Small Molecules					
Fluorodeoxyglucose (8/1999)	FDG	Proliferating Cancers	Functional	^{18}F	PET
Pentetreotide (11/1998)	Octreoscan	NET	Somatostatin Receptor	^{111}In	SPECT
1,4,7,10-tetraazacyclodecane-1,4,7,10-tetraacetic acid (DOTA)-octreotate (6/2016)	DOTATATE	NET	Somatostatin Receptor	^{68}Ga	PET
PSMA-11 December 2020	Ilucix	Prostate Cancer	PSMA	^{68}Ga	PET
DCFPyI (5/2021)	Pylarify	Prostate Cancer	PSMA	^{18}F	PET
^{18}F -rh-PSMA-7.3 (6/2023)	Posluma	Prostate Cancer	PSMA	^{18}F	PET
Pafolacianine (11/21)	Cytalux	Lung and Ovarian Cancers	Folate Receptor	NIR	FGS
Antibodies					
B72.3* Murine IgG (1992)	Oncoscint	Colorectal Cancer	TAG-72	^{111}In	SPECT
NR-LU-10* Murine Fab (1996)	Verluma	Small Cell Lung Cancer	CEA	$^{99\text{m}}\text{Tc}$	SPECT
NP-4 Fab* (1999)	Arcitumomab	Colorectal Carcinoma	CEA	$^{99\text{m}}\text{Tc}$	SPECT
7E11-C5.3* Murine IgG (1996)	ProstaScint	Prostate Cancer	PSMA	^{111}In	SPECT

TABLE 2 | Generations of monoclonal antibodies to TAG-72: Their source and applications.

Anti-TAG-72 MoAb	Generation	Type	Applications (patients injected)	References
B72.3	1st	Murine IgG	SPECT Phase I and II RIGS (N = 805)	[41, 60]
CC49	2nd	Murine IgG	Phase I and II RIGS/ADCS SPECT—Pilot (N = 459)	[41, 61, 62]
CC49	2nd	Fab'	Preclinical MicroPET/CT	[62]
CC83	2nd	Murine IgG	Pilot—RIGS/ADCS (N = 17)	[63]
HuCC49	3rd	Bioengineered IgG	Preclinical Fluorescent Imaging	[64]
HuCC49Δ(CH2)	3rd	Bioengineered Chimeric IgG From CC49	Pilot—RIGS/ADCS (N = 20)	[65–68]
3E8	4th	Bioengineered Humanized IgG From CC49	Preclinical Pharmacokinetics	[69]
AVP04-7-PEG	5th	Bioengineered Humanized scFv and Diabody From CC49	Pilot - PET (N = 6)	[50, 70, 71]
3E8.scFv.Cys	5th	Bioengineered Humanized scFv From 3E8	Preclinical FL Imaging	[72]
ENL-210	5th	Bioengineered Humanized scFv—diabody -tetrabody From 3E8	Preclinical Imaging	[49]

binding by Fc receptors of intact mMoAbs can lead to decreased TBRs [48].

Enzymatic digestion removes the constant regions from the mMoAb to yield smaller Fab' and F(ab')₂ fragments that exhibit rapid tumor penetration and increased renal clearance without altering antigen binding. The bioengineered single-chain fragment variable (scFv) fragments, containing a variable light chain (VL) and a variable heavy (VH) chain, require a linker molecule for stability and are easier to produce [49]. The scFv can give rise to multivalent diabody, triabody, tetrabody, and minibody (scFv-CH3) fragments with the same avidity, affinity, and optimal pharmacokinetics (Figure 2). There are even smaller, 15 kDa, single domain VH chains or nanobodies, small peptides, and chemicals that are potential PLs for molecular imaging. These bioengineered PLs retain the high affinity and avidity of the intact mMoAb while providing improved renal clearance and tumor penetration. The result is a better TBR than the parent mMoAb and, thus, a better EODT image [48]. In cases where there is a need to increase the serum half-life of smaller PLs to optimize tumor uptake and reduce renal clearance, this is

accomplished by adding discrete sizes of polyethylene glycol to the PL [12, 50].

Small molecules such as the glucose analog ^{18}F -fluorodeoxyglucose (FDG) and fibroblast-activating protein inhibitor (FAPI) have a biological half-life measured in minutes, facilitating their use for preoperative molecular imaging (Figure 2). PET/CT, using the radionuclide-labeled glucose analog ^{18}F -FDG as the PL, is the current “go-to” for hybrid molecular imaging for non-small cell lung cancer, head and neck cancers, and lymphomas. ^{18}F -FDG-PET/CT is helpful in selected CRC cases for identifying metastases; however, its low specificity minimizes its use in preoperative imaging [51, 52]. The increased uptake of ^{18}F -FDG by inflamed tissue, wound healing, and infections results in false positive images, whereas slow-growing tumors exhibit no increase in ^{18}F -FDG uptake [53].

Although not FDA-approved, PET and PET/CT using radionuclide-labeled FAPI show promise as a replacement for ^{18}F -FDG in preoperative imaging of CRC. Upregulation of fibroblast-activating protein (FAP) expression by cancer-associated fibroblasts occurs in 90% of primary and metastatic

carcinomas [54]. In the case of CRC, the improved TBR of ^{68}Ga -FAPI PET/CT over ^{18}F -FDG-PET/CT leads to improved identification of primary and recurrent disease and in the detection of lymph node metastases [55]. Similar head-to-head studies of other tumors demonstrate that EODT using FAPI is equal to or superior to FDG in many tumors, including CRC. However, neither FDG nor FAPI binding is cancer-specific. False positive imaging occurs in wound healing and various diseases characterized by fibrosis, e.g., cirrhosis, healing myocardial infarcts, and autoimmune diseases. False negative imaging is associated with tumors lacking accumulation of cancer-associated fibroblast, e.g., leukemia, lymphomas, and multiple myeloma [54].

Even though there are multiple FDA-approved MoAbs for therapy, there is only a limited number for imaging. Many previously approved imaging products are no longer on the market in the United States [56]. Many of the early SPECT-related PLs were taken off the market, partly due to the increasing use of ^{18}F -FDG-PET and ^{18}F -FDG-PET/CT and issues with image quality (Table 1). As noted earlier, developing new PLs for neuroendocrine and prostatic carcinomas is reestablishing the central role of preoperative molecular imaging in providing an accurate EODT road map [32, 57]. Based on decades of clinical rather than preclinical results, we propose that the same success can be attained for EODT assessment in CRC using newer versions of PLs specific for the tumor-associated glycoprotein-72 antigen (TAG-72) and for the carcinoembryonic antigen (CEA), a member of the carcinoembryonic antigen cell adhesion family of molecules (aka CEACAM5). The nonspecific tumor-specific expression of TAG-72 and CEA is associated with 80%–95% of CRC primary and recurrent tumors. Both are large membrane-bound glycoproteins found in a diverse group of carcinomas and a few non-malignant conditions. However, except for secretory endometrium with TAG-72, it shows little or no expression in normal tissue [8, 58].

TAG-72 is a mucin-like glycoprotein biomarker for CRC and other adenocarcinomas. TAG-72 has a single protein core with extensive O-linked glycosylation that accounts for 80% of its molecular weight of 1,000 kDa [59]. The function of TAG-72 is unknown but may be capable of inhibiting the immature dendritic cells in the tumor and in tumor-draining lymph nodes [14]. Immunohistochemical (IHC) staining demonstrates TAG-72 in cytoplasmic secretory vacuoles on the extracellular matrix's plasma membranes, luminal secretions, and mucin lakes [14].

The last 30 years saw multiple generations of mMoAbs developed as PLs for TAG-72 (Table 2). Over 1,000 patients have safely received one of several generations of mMoAbs to TAG-72 in clinical studies of various carcinomas (Table 2). [41] The first-generation anti-TAG-72 mMoAb B72.3 received FDA approval for SPECT imaging. Numerous single-institution and multicenter clinical trials of primary and recurrent CRC for radioimmunoguided surgery (RIGS) used B72.3 [73–77]. CC49 is the second generation mMoAbs to TAG-72 and has an improved affinity and avidity for TAG-72 compared to B72.3 [61, 78–80]. IHC staining with CC49 demonstrates TAG-72 in

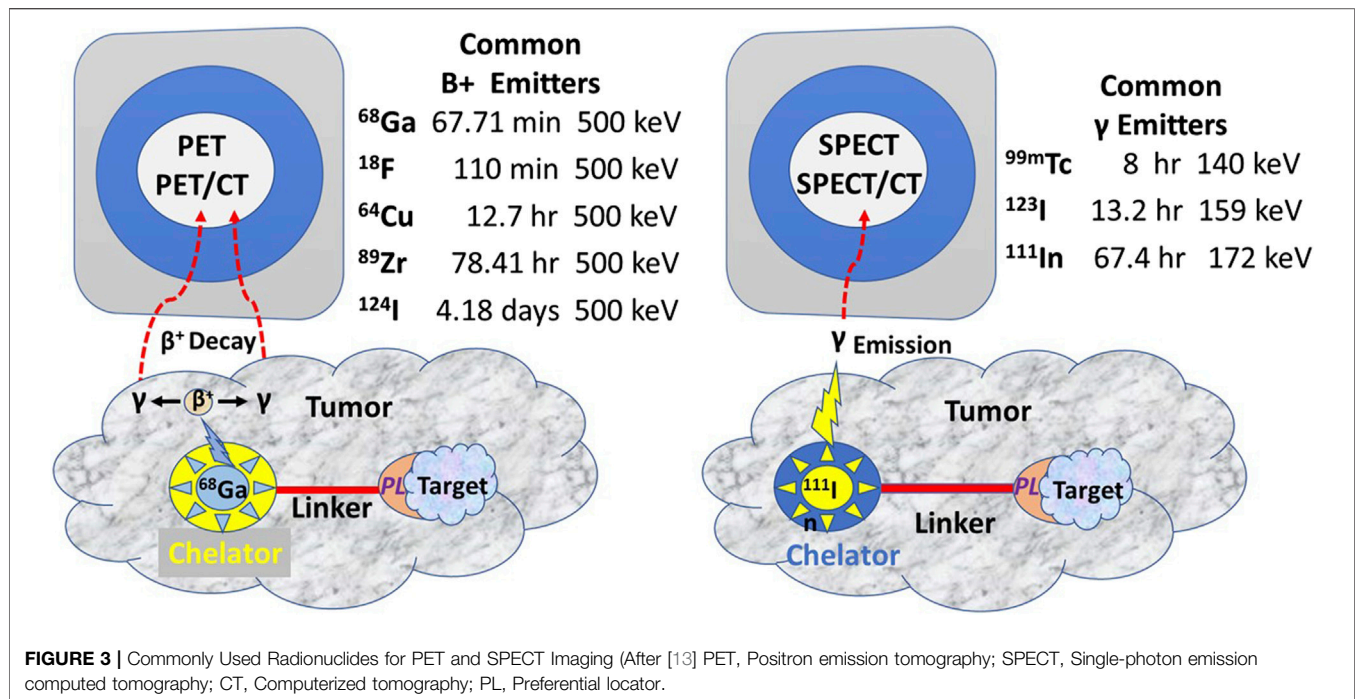
86% of primary CRC tumors and 96% of recurrent tumors. CC49 provides the starting material antibody fragments and bioengineered derivatives of scFv, which are in preclinical and early phase I/II studies (Table 2). The use of mMoAbs to TAG-72 has been directly correlated to patient overall survival in the setting of RIGS or what we now refer to as Antigen-Directed Cancer Surgery (ADCS), but not in the context of preoperative PET/CT imaging [42].

Over the last 40 years, numerous anti-CEA mMoAbs were developed and used for serum detection, IHC staining, preoperative and intraoperative imaging, radiation therapy, and immunotherapeutics. The mMoAbs to CEA bind to one of the nine domains (A1, B1, A2, B2, A3, B3, and N) that form the 79 kDa core protein [81–86]. The last decade has steadily progressed from preclinical to the current phase III clinical trial using mMoAb SGM-101, a chimeric IgG in the A2 domain of CEA core protein. Later studies focus on FSG, which requires intraoperative imaging resources [87]. The results of a Phase II trial demonstrated tumor involvement of the peritoneum, superficial lymph nodes, and surgical margins that improved real-time surgical decisions. In contrast to fluorescence imaging, a recent study reported using a humanized chimeric mMoAb recognizing the A3 domain of CEA for preoperative PET/CT imaging of 20 patients with either gastric, colorectal, medullary thyroid, or neuroendocrine carcinoma [88]. Although the mMoAb had a high affinity for CEA, the authors concluded that the mMoAb is optimal for imaging patients with locally advanced rectal carcinoma. This last study highlights the impact of PLs on the endpoints selected for clinical studies. However, numerous ongoing clinical trials use various PLs for imaging and therapy of solid tumors [56, 89].

Tracer Molecules

The tracer molecule (radionuclide or fluorophore) linked to the PL bound to the target molecule produces the signal (Figure 3). The molecular relationships among the components of the radiopharmaceuticals—the PL, the tracer, the bifunctional chelator, and the linker—are critical to optimizing the TBR needed for an accurate EODT assessment. Optimizing results begins by closely matching the linked radionuclide's half-life with the PL's biological half-life.

In contrast to iodine radionuclides, radiometals used for PET and SPECT require a chelator to form a stable complex with the metal ion to prevent metal loss after the intravenous injection and form a bifunctional complex by linking to the PL for injection. Chelators reduce the harsh conditions for labeling a PL with ^{18}F . A linker molecule joins the chelated radionuclide to the PL (Figure 3). Radionuclide tracers for PET imaging undergo B^+ decay, yielding two high energy gamma (γ) rays 180° apart. However, the improved sensitivity of the PET, and thus the better EODT preoperative roadmap, is more a function of the instrumentation rather than the number of gamma rays emitted. High-energy radionuclides have far greater tissue penetrance, allowing for imaging and detection at a greater distance from the source and for detecting small sources.



The TBR is the critical variable allowing intraoperative detection and imaging of small (<5 mm diameter) gamma-positive tissue. In our experience, this requires the physical half-life of the radionuclide (referred to as radionuclide decay $T_{1/2}$) to be at least five times that of the biological half-life due to clearance from normal tissue [90, 91]. PET and PET/CT use a high-energy radionuclide-bound PL for preoperative molecular imaging. In the initial EODT assessment for CRC cases, we propose using ^{124}I to label the PL. This high-energy radionuclide has a physical half-life of 4.2 days and a biological half-life of approximately 61 days, which allows for imaging over several days and optimizing the TBR for a more accurate EODT roadmap. The intraoperative EODT assessment for CRC currently calls for using a low-energy radionuclide. We recommend ^{123}I , bound to the same PL used for the “roadmap” for intraoperative imaging and detection. ^{123}I has a physical half-life of 13.2 h compared to a biological half-life of 120–138 days if unbound. The ease of labeling a PL with ^{124}I for PET imaging and ^{123}I for intraoperative EODT assessment should not alter the affinity or the avidity of the PL. To further optimize the TBR while maintaining the avidity and affinity of the PL, we propose an EODT assessment of CRC using the chimeric anti-TAG-72 MoAb, HuCC49 Δ CH2, that is currently available. HuCC49 Δ CH2, with its complementarity determining region (CDR)-grafted humanized domain-deleted CC49 MoAb, was safely administered to 20 patients with recurrent CRC [91]. Pharmacokinetic studies indicate that its physical half-life is 1.34 days, its biologic half-life is 12.8 days, and renal excretion accounted for over 66% of the clearance [66].

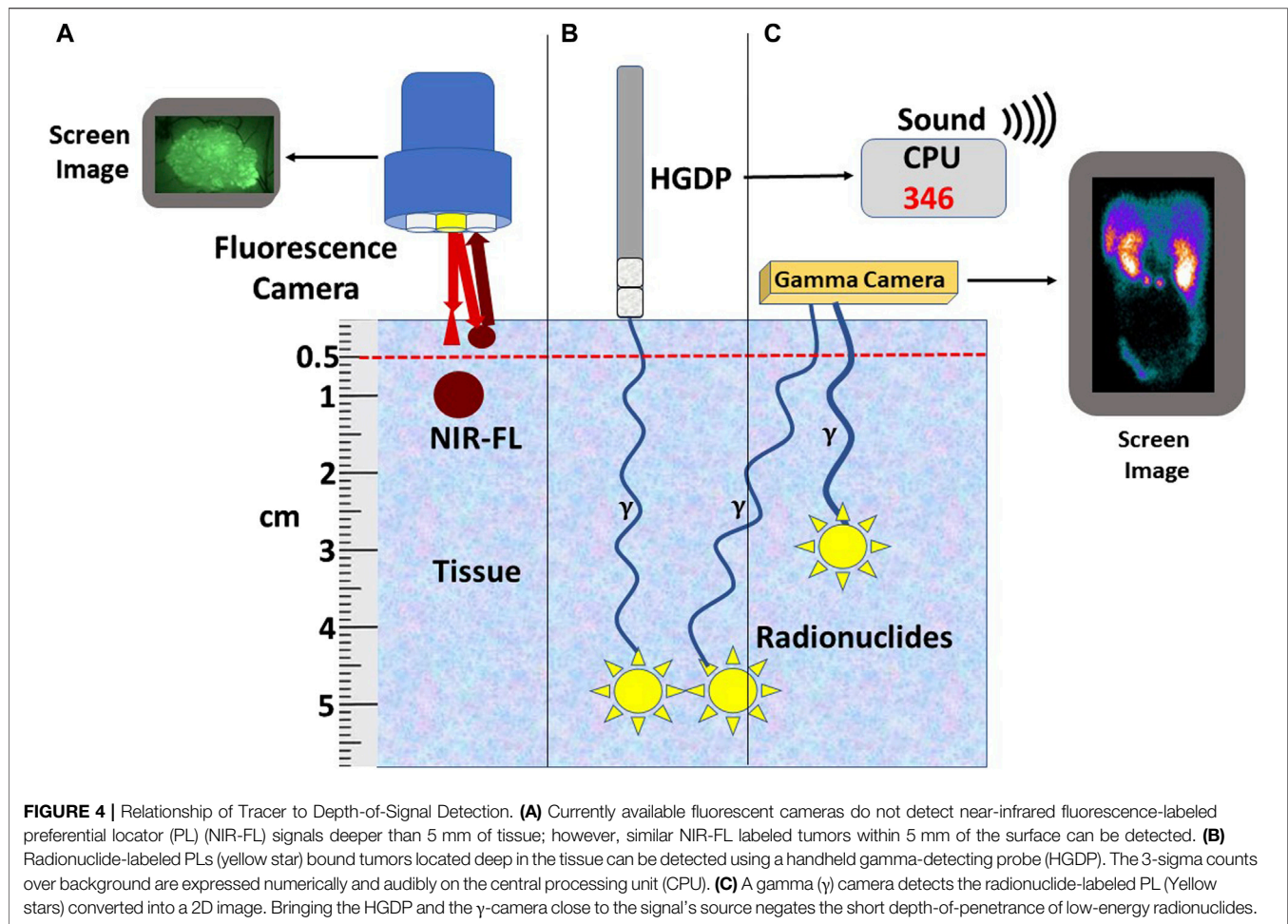
Preclinical and clinical research into fluorophore-guided surgery is expanding [6, 92–103]. An international, multicenter, phase III clinical trial for intraoperative EODT

assessment in primary and recurrent CRC cases is underway [104]. The study employs a near-infrared (NIR) fluorophore (carbocyanine dye (BM105) labeled anti-CEA mMoAb (SGM-101) for real-time intraoperative assessment for positive surgical margins. The problem of positive margins varies with the tumor type [9] and occurs in over 15% of all resected cancers [105]. This procedure also has the advantage of real-time assessment for occult carcinomatosis [106]. However, the inability of NIR light to penetrate beyond 5 mm (Figure 4) minimizes its ability to detect tumor-involved regional and extra-regional lymph nodes seen on preoperative images. Current FDA clinical approval of only two NIR dyes in the 700–900 nm range—indocyanine green and methylene blue—must be expanded to include other NIR dyes whose emission wavelength has deeper tissue penetration and a better TBR. In addition, the future holds great promise for combining both types of tracers on the same PL [102, 107, 108].

Intraoperative Imaging and Detection of the Tracer Signal

There is ongoing research and development of medical devices for intraoperative imaging and detecting radionuclides and NIR fluorophores. Further proof of the proposed concept for intraoperative EODT assessment is well underway with the FDA approval of ^{68}Ga -PSMA-11 for primary and recurrent prostate cancer [33] and with the current phase III trial with the NIR fluorophore labeled anti-CEA SGM-101 [92], as well as the fluorescence-guided ovarian and lung cancer surgery using Pafolacianine [100, 109].

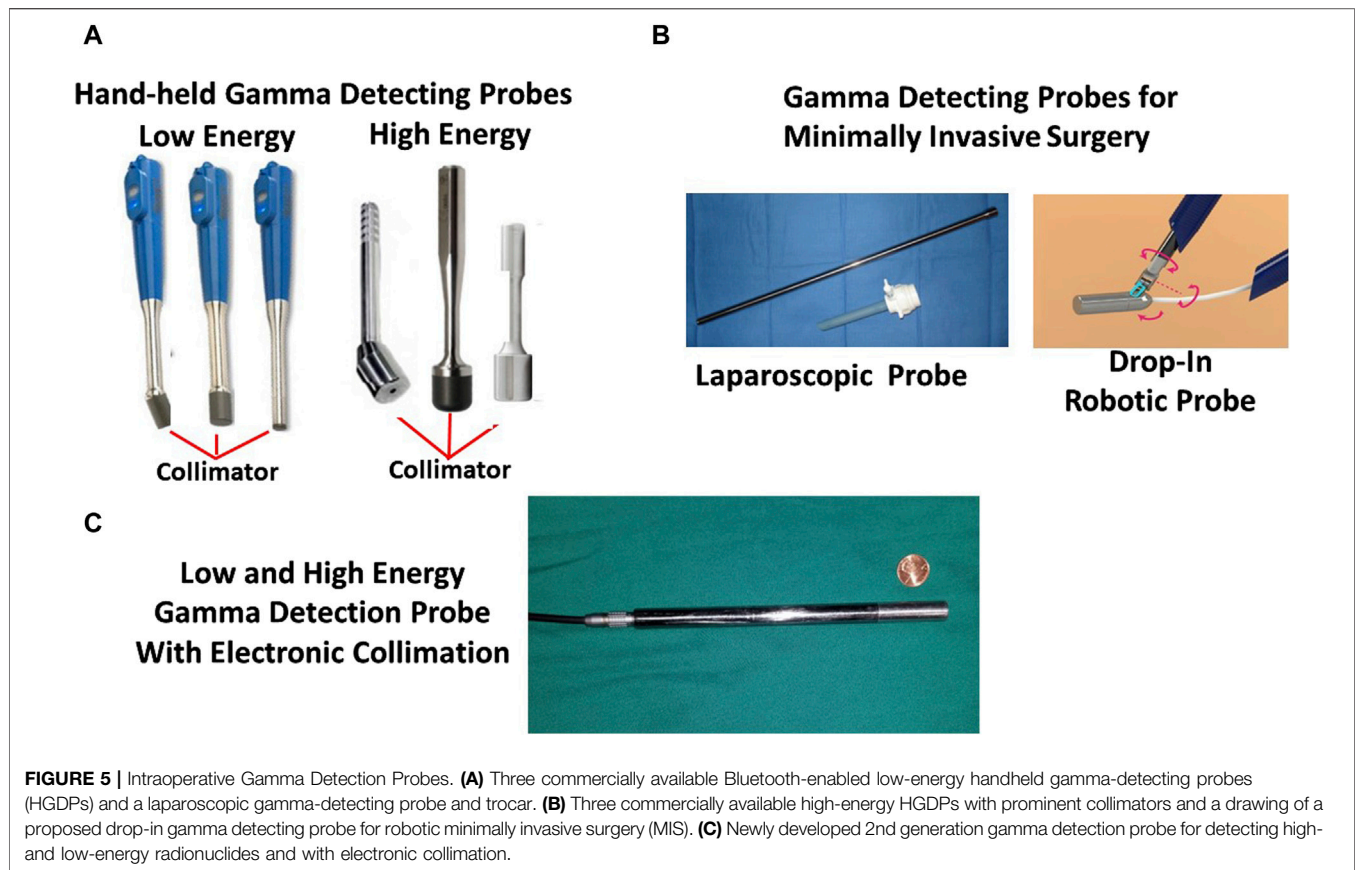
The type of equipment is defined by the type of surgery—open vs. minimally invasive—and by the depth of the tracer signal



within the tissue (Figure 4). By themselves, PET and SPECT molecular imaging have limitations in detecting DIT smaller than 5 mm in the greatest dimension. The primary reasons are that the detectors are several centimeters away from the source and have a relatively low sensitivity to detect low-energy emitted gamma rays [103]. Thus, to find gamma-positive tissue smaller than 5 mm requires a detector to be close to the source. The introduction of the sentinel lymph node biopsy as the standard of care for several cancers and the ability of a handheld gamma-detecting probe (HGDP) in direct contact with the tissue led to the development of a wide range of probes and control units (Figure 5). Many of the current low-energy gamma-detecting probes are Bluetooth-enabled. HGDPs for high-energy radionuclide detection are not ergonomic due to additional shielding that increases probe weight, restricting them to open procedure use. The central processing unit, or console, provides a digital count rate and audio output that may vary its pitch based on the count rate. The control unit uses a three-sigma criterion—the baseline count plus three times the square root of the baseline or greater to provide a positive count [90, 110]. We designed the next-generation of gamma probes (e.g., handheld and MIS compatible) capable of detecting low and high-energy radionuclides using electronic collimation (U.S. Patents Nos. 11,467,295 and 11,562,454) that

improves probe sensitivity by eliminating the need for physical collimation [111]. Optimal intraoperative EODT assessment occurs with the gamma-detecting probe, capable of being placed close to the source of the signal, used in conjunction with a portable small or portable large field-of-view gamma camera. Reviewed by [112] In addition to providing the required field-of-view, resolution, and sensitivity, the surgeon needs real-time monitoring and no delay in acquisition and display. The handheld cameras have the same disadvantage as the gamma probes in that they depend on the ability of the user to position the probe toward the source correctly. We have used a portable SPECT gamma camera (Ergo) in conjunction with HGDPs for six cases with recurrent gastrinoma that demonstrated 100% pathologic correlation with the imaging findings [10]. Similar results occur in SPECT imaging of ^{99m}Tc -Sestamibi for parathyroid adenomas [113].

Lauwerends et al. [97] defined fluorescent-guided surgery (FGS) as “an optical imaging method that provides real-time guidance for delineation of [tumors] during surgery, with higher sensitivity than direct visual inspection and palpation.” As with gamma probes and cameras, near-infrared (NIR) fluorescent imaging systems provide both ergonomic and real-time information to ensure adoption by surgeons. In the CRC setting, these systems assess surgical margins,



lymph nodes, and peritoneal surfaces for occult-tumor in EODT assessment of CRC [87, 114]. These include systems for open, laparoscopic, and robotic FGS procedures. Commercial systems for FGS vary in their features. Reviewed in [110] As indocyanine green (ICG) is the only FDA-approved NIR fluorescent dye useful for FGS studies, various excitation light sources—laser diodes and light-emitting diodes—include NIR bandwidth. Each system varies according to its working distance, field of view, image contrast, and quality. Charge-coupled device cameras provide high-resolution and cost-efficient means of capturing the emitted photons and provide qualitative rather than quantitative EODT images. Ongoing development of new sensors indicates that the improved depth of fluorescent signal detection is greater than the accepted 5 mm value.

Proofs of the Concept

Our clinical studies demonstrate that the proposed approach (Figure 1) works. By providing the surgeon with an accurate assessment of the EODT intraoperatively (Figures 6–8), the surgeon is more likely to achieve a complete R0 resection, improving patient survival (Figures 9, 10).

An Accurate Assessment of EODT Provides Added Value to the Surgeon and the Patient

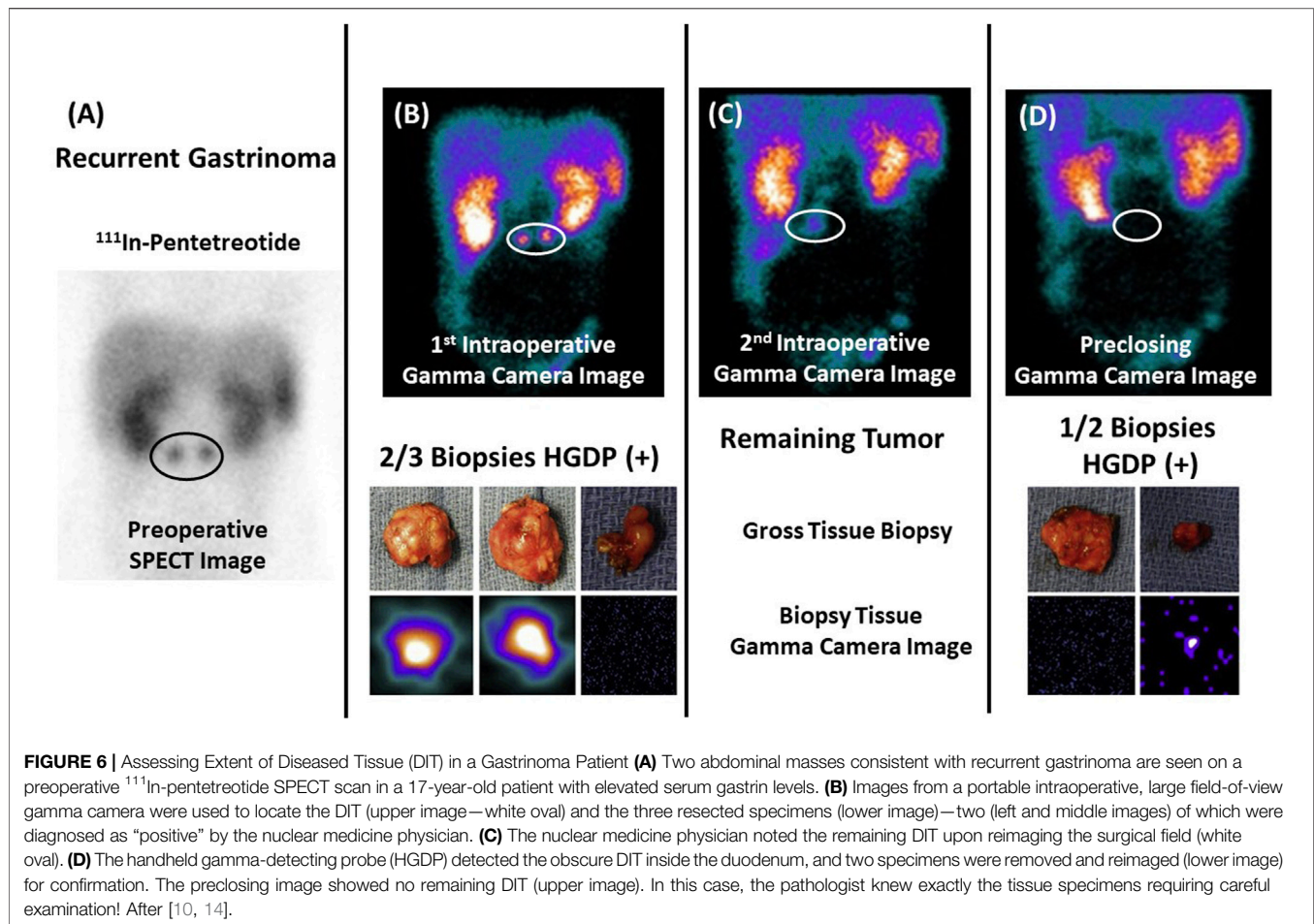
In the case of neuroendocrine carcinomas, Figure 6, we used the same radionuclide labeled PL (^{111}In -pentetretotide) for the

preoperative and intraoperative imaging in conjunction with an HGDP for intraoperative detection of the gastrin-secreting tumor. Figure 6 demonstrates our proposed approach's ability to assess the EODT from the initial preoperative imaging to intraoperative detection and imaging prior to closing [10].

Pathologist knew exactly the tissue specimens requiring careful examination! (After 10 and 58).

Increasing Detection DIT in Colorectal Carcinoma

In the case of primary and recurrent CRC cases, inadequate preoperative imaging hampered our earlier clinical studies. A careful and detailed exploration of the abdomen and pelvis using an HGDP partially overcame the lack of an intraoperative gamma camera. Although this approach had a significant impact on the surgical procedure itself, having a “large field” gamma camera intraoperatively to demonstrate diseased tissues would have impacted patient morbidity and mortality. This conclusion is based on the fact that, under the term radioimmunoguided surgery (RIGS), we repeatedly demonstrated the truism “that it is what is left behind kills the patient, not what the surgeon takes out” and that traditional surgical procedures leave a lot of DIT behind (Figures 7–10). Achieving an R0 resection is the most important variable associated with recurrence and long-term survival; however, it may not be possible due to the extent and location of DIT.



The first step in assessing the EODT is locating DIT as defined by the binding of the PL. Two early studies demonstrate this premise. **Figure 7** demonstrates the accuracy of ADCS (RIGS), using ¹²⁵I-CC83, a 2nd generation mMoAb to TAG-72, for DIT in 17 patients with CRC [63]. This small study demonstrated that the sensitivity of the preoperative CT scan was only 44%, a finding that tends to support the conclusion by Brouwer et al. [120] that the “accuracy of clinical lymph node staging in colorectal cancer patients is about as accurate as flipping a coin.” It also demonstrated that while the more subjective, traditional surgical visual and palpation performed better than the CT scan in assessing EODT, the sensitivity of ADCS to detect tumors was 100%, but the presence of “false positive” findings decreased its positive predictive value.

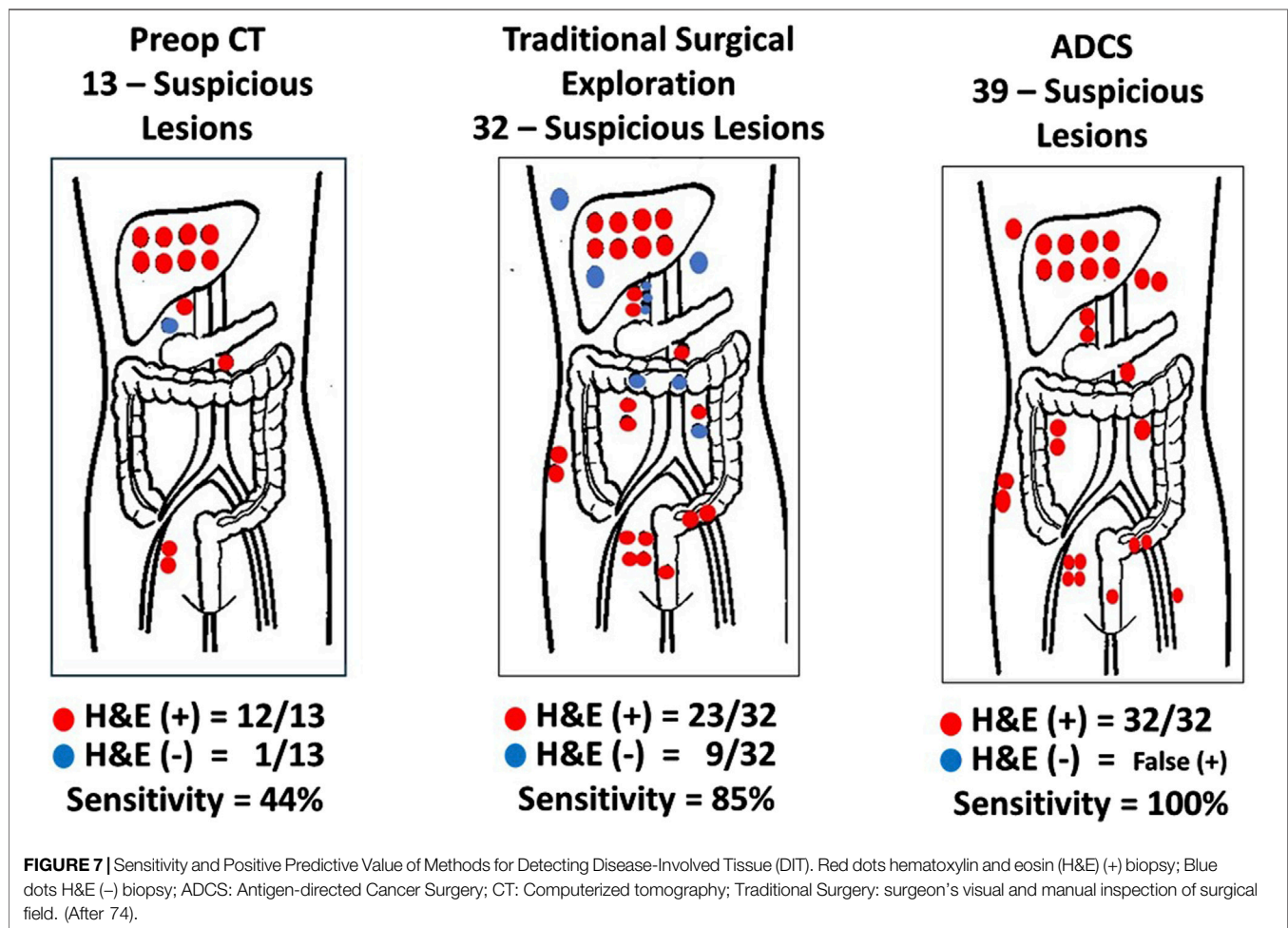
Mirroring the results of **Figures 7, 8** depicts the results of ADCS of CRC using ¹²⁵I-labeled CC49, the principal primary 2nd-generation mMoAb to TAG-72, for intraoperative detection of DIT in CRC patients [121]. The figure demonstrates that the extent of CRC involves extra-regional tissue in primary and recurrent cases exceeds textbook examples. The surgeon’s exploration using traditional techniques (i.e., visual inspection and palpation) and the HGDP detected the liver’s metastases equally. “The issue is extra-regional tissue.” In this case, the disease involved extra-regional or “non-anatomic” draining

lymph nodes that do not follow the usual arterial and venous vessels and, therefore, are unexplored during traditional exploration, including clusters of perirenal, retroperitoneal, and small bowel mesenteric nodes. Occult metastases occurred in the abdominal wall, omentum, pelvic, sacral, and iliac nodes. Many of these lymph nodes are too deep for detection by fluorescence-guided surgery.

A preop roadmap map is needed to ensure that many nodal locations go unexamined today during routine open or MIS procedures. In the case of primary and recurrent CRC, the EODT goes well beyond what traditional surgical approaches explore. We and others have previously reported that assessing EODT using our approach resulted in a change in the extent of surgery in up to a third of primary and recurrent CRC cases using the first and second generation mMoAbs to TAG-72 [115, 122–125] and up to half of primary and recurrent CRC cases.

Colorectal Carcinoma as an Exemplar of DIT

What is disease-involved tissue (DIT)? To answer this question, one needs to understand that there is an ongoing debate about what an actual false positive lymph node is, which is HGDP (+) but lacks tumor cells on a single H&E-stained section for routine microscopic examination. The first proof that these lymph

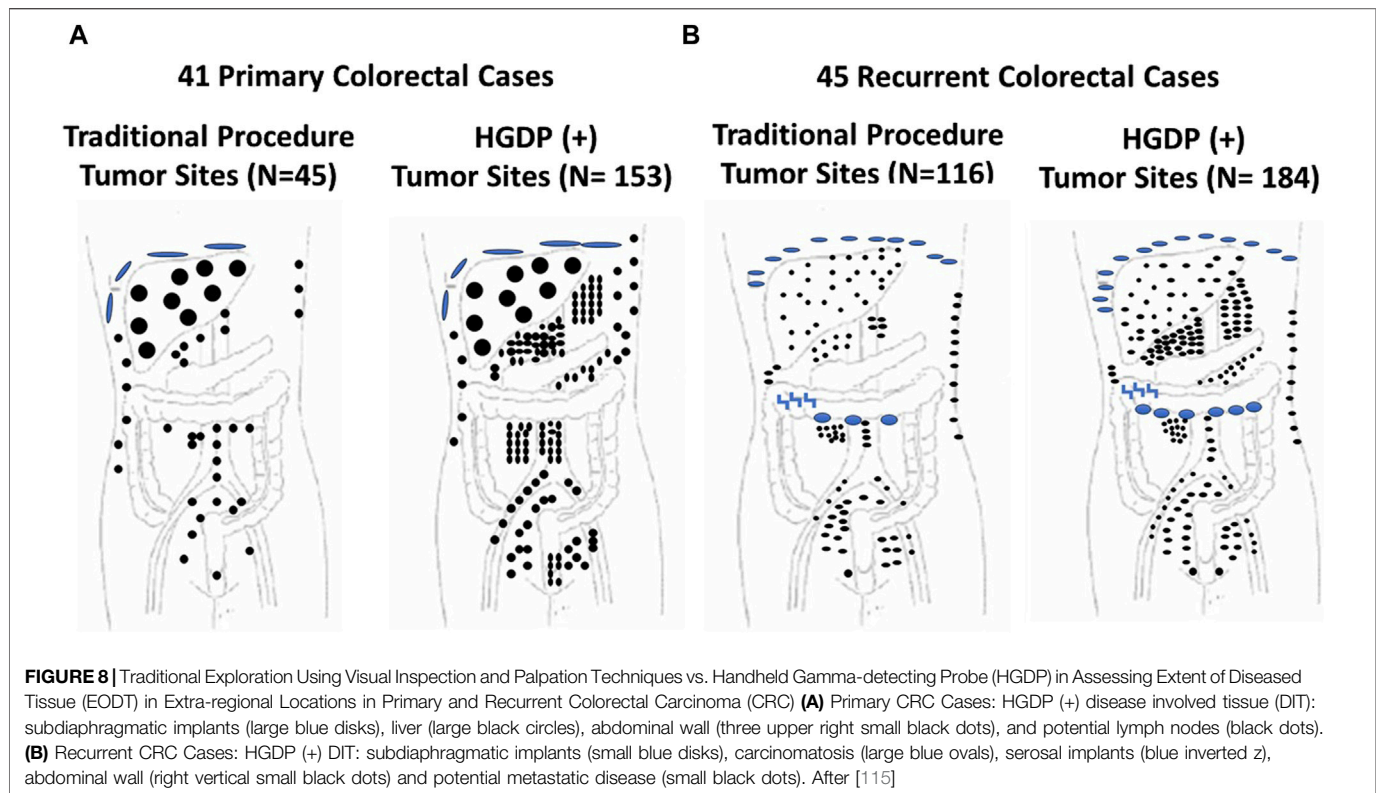


nodes are indeed DIT comes from IHC staining demonstrating TAG-72 expression in the germinal centers of these nodes, along with autoradiography demonstrating ^{125}I -CC49 similar localization [40]. Some authors say yes, it is a false positive [126–128], while others say not so fast [117, 119, 129–134]. The evidence is conflicting. In a previously reported study of 599 tissue specimens from 92 patients with primary or recurrent CRC [14], we found tumor cells in 134 of 145 (92.5%) non-lymphoid, HGDP (+), and DIT submitted for routine pathology. However, only 71 of the 452 (15.7%) HGDP (+) lymph nodes contained tumor cells on routine H&E-stained slides. These results led us to explore the inherent variables associated with routine pathologic examination of lymph nodes for metastatic tumor cells. Sampling error and detection sensitivity are the two most significant variables. Both are associated with the unequal distribution of tumor cell clusters within a lymph node. Identifying these tumor clusters is helped by using additional slides for H&E and IHC staining; however, they do not eliminate the impact of these variables. Additional sectioning into the lymph node-containing paraffin block and cytokeratin IHC staining identified tumor cells in 102 of 172 (59%) pStage

I/II CRC cases. Using a pseudotumor model, we examined the ability of the light microscope to detect tumor cells. We found that cytokeratin IHC staining increased the detection level compared to H&E-stained sections evaluated by three pathologists. It also demonstrated that cytokeratin IHC staining increased microscopic detection sensitivity from <1 tumor cell in 2000 mononuclear cells to <1 in 20,000. Additional detection sensitivity is available using molecular techniques [130–132] and tissue culture [133]. However, the reality is that additional sectioning, cytokeratin IHC staining, molecular genetics, and tissue culture are too expensive and time-consuming for routine use. The actual answer to the clinical importance of pathology-negative HGDP (+) DIT comes from our patient outcome data [117].

Clinical Relationship between pStage RO and DIT in ADCS of Colorectal Carcinoma

The literature contains numerous articles that describe various surrogate markers of tumor progression and patient survival. Among these are studies that report that the presence of otherwise undetected occult tumor cells in regional and extra-regional lymph nodes is associated with a worse prognosis for



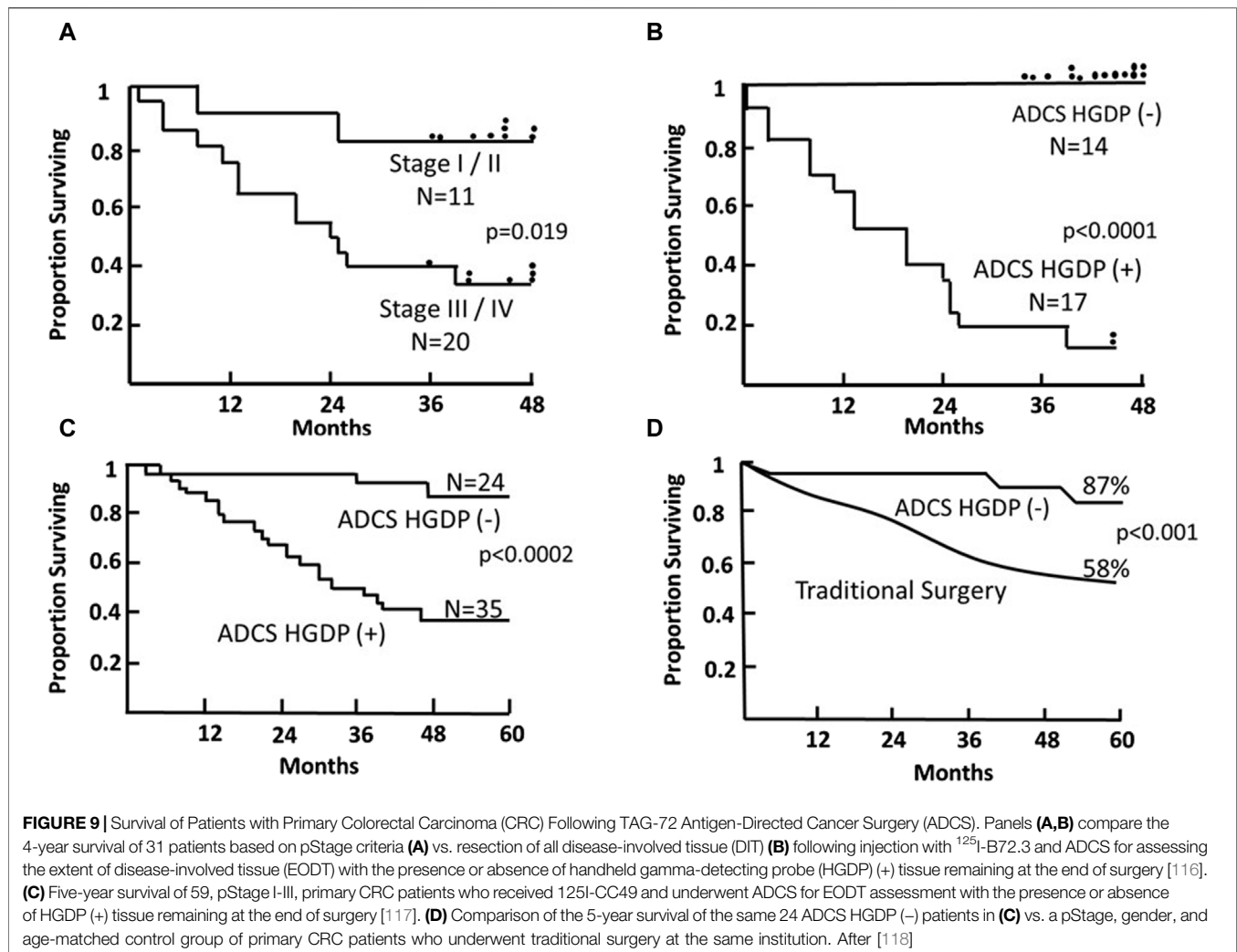
CRC patients [119, 130, 134]. Our ADCS prospective data demonstrates the significant impact of assessing the EODT in patients with either primary or recurrent colorectal carcinoma on their overall survival (**Figures 9, 10**). The Kaplan-Meier plots demonstrate several significant issues. First, there are two distinct groups of patients with primary or recurrent CRC to which TAG-72 ADCS indicates significant survival variability. **Figure 9** demonstrates that in the short term (4-5-year), removing all DIT [i.e., TAG-72 HGDP (+)], regardless of the preferential locator (B72.3 or CC49 mMoAb), provides a significant survival advantage. It also identifies patients who will require adjuvant therapy after surgery **Figure 10C** depicts the long-term survival of 92 patients with primary CRC injected with I-124 CC49 and CC83 and followed for 125 or more years. Secondly, based on pathologic features, current staging guidelines must include molecular variables. The data in **Figure 9** suggest that patient survival can significantly vary from the parochial strict anatomic approaches taken by surgery and pathology alone. Understanding the role of the immune response to TAG-72 and other tumor-associated factors will be critical, and the ability to sample the specific tissues of interest using ADCS will help to facilitate this [14].

Conclusion

A “systems engineering” concept for assessing the EODT in solid tumors coupled with a multidisciplinary team is essential in today’s management of patients with primary or recurrent disease. Although enrollment of our CRC patients occurred in the late 1980s through the 1990s, the data presented here are

one-of-a-kind. It is prospective and includes long-term patient follow-up. Very few studies of TAG-72 expression and ADCS were performed, with few exceptions since we stopped accruing patients. Our studies depended on the use of a family of newly designed handheld gamma probes (Neoprobe, Corp—now Devicor® Medical Products, Cincinnati, OH), a family of newly developed mMoAbs to TAG-72 (provided by Jeffery Schlom, Ph.D., CCR, NCI) and the faculty and staff of The Ohio State University, College of Medicine. Although the data presented here comes from our work, similar significant survival results occurred in a multicenter trial [102]. What is evident from the data in **Figures 9, 10** is that there is a critical need for preoperative EODT assessment that provides surgeons and the multidisciplinary team (surgeon, nuclear medicine, and medical oncology) with accurate information upon which to base their clinical decisions. SPECT/CT and PET/CT were unavailable when we conducted our TAG-72 ADCS studies; however, we were frustrated with the preoperative CT imaging that gave us an inaccurate impression of the patient’s EODT.

The proof-of-concept study involving six cases of gastrinoma used ^{111}In -pentetreotide for preoperative and intraoperative imaging using a portable large field-of-view gamma camera and a commercial HGDP [10]. As this study demonstrated, intraoperative EODT assessment requires the simultaneous use of a portable gamma camera and an HGDP. **Figure 11** envisions that portion of **Figure 1** following the decision for surgery in a case of CRC. This thought experiment uses a currently unavailable PL but current state-of-the-art preoperative and

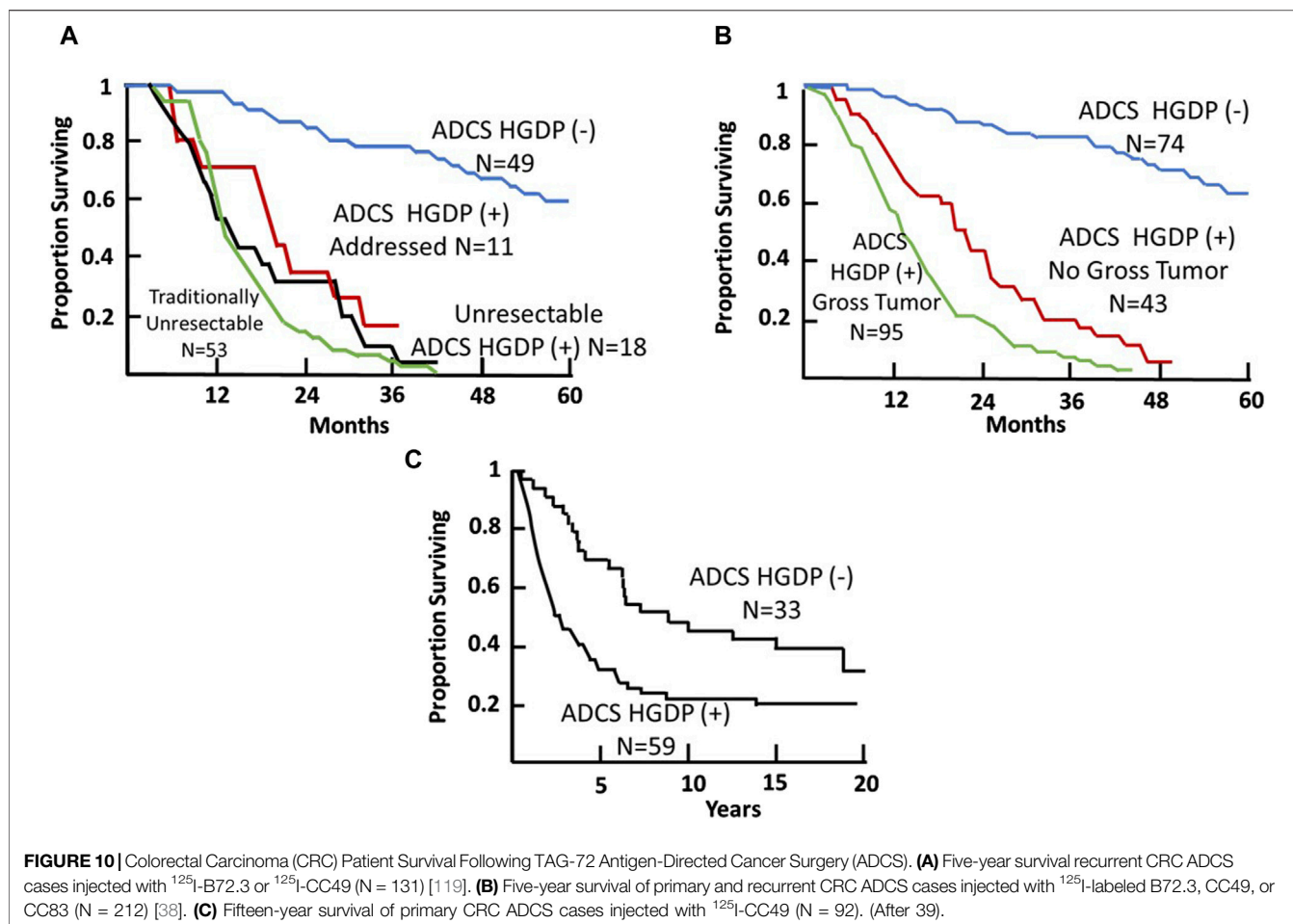


intraoperative imaging technologies and gamma detection probes (e.g., HGDP, laparoscopic, and robotic).

Our proposed concept calls for a portable gamma camera and a gamma detection probe to be used intraoperatively and together rather than in isolation. Bringing instrumentation for intraoperative EODT assessment into the 21st century requires the development of new gamma cameras and probes for open and MIS surgery capable of imaging and detecting “pan-energy” radionuclide tracers. This development is needed because PLs labeled with high energy, short half-life radionuclides allow PET/CT roadmaps to provide preoperative and intraoperative imaging. A single PET/CT generated pre- and intraoperative EODT “roadmap” saves time and money while providing the surgeon and the patient with added value results. However, for EODT to become clinically successful requires continued development of both old and new PLs. PSMA-11 and DOTATATE are our role models for a successful PL for EDOT and would be a great starting place for the clinical approach demonstrated in **Figure 11**. Clinical grade chimeric and humanized MoAbs, including humanized domain deleted CC49 to TAG-72, are available, and there is ongoing research and

development of small fragments for possible EODT assessment. In addition to CRC, MoAbs to TAG-72 are applicable for EODT assessment in most cases of adenocarcinomas of the ovaries, endometrium, breast, prostate, pancreas, stomach, and lungs, opening a new era of multidisciplinary oncology care-based on accurate preoperative and intraoperative EODT imaging and detection [34].

Thirdly, in the case of recurrent CRC (**Figures 10A, B**), as with primary CRC, TAG-72 ADCS can provide a significant survival advantage to a distinct group of patients. Panel A indicates that we took all comers for our clinical studies [73]. At least 40% (53/131 patients) enrolled were unresectable by ADCS but were addressed by traditional surgery. Another 29 (22%) of patients were found to be unresectable and had HGDP (+) tissue remaining at closing. For the group of 49 patients (37%), there was a significant survival advantage ($p < 0.0001$) as compared to the group of unresectable cases. Panel B depicts the 5-year survival of the 212 primary and recurrent CRC patients who underwent ADCS with either B72.3, CC49, or CC83 mMoAbs over 14 years [38]. Again, we see three distinct populations. The poorest survival is associated with

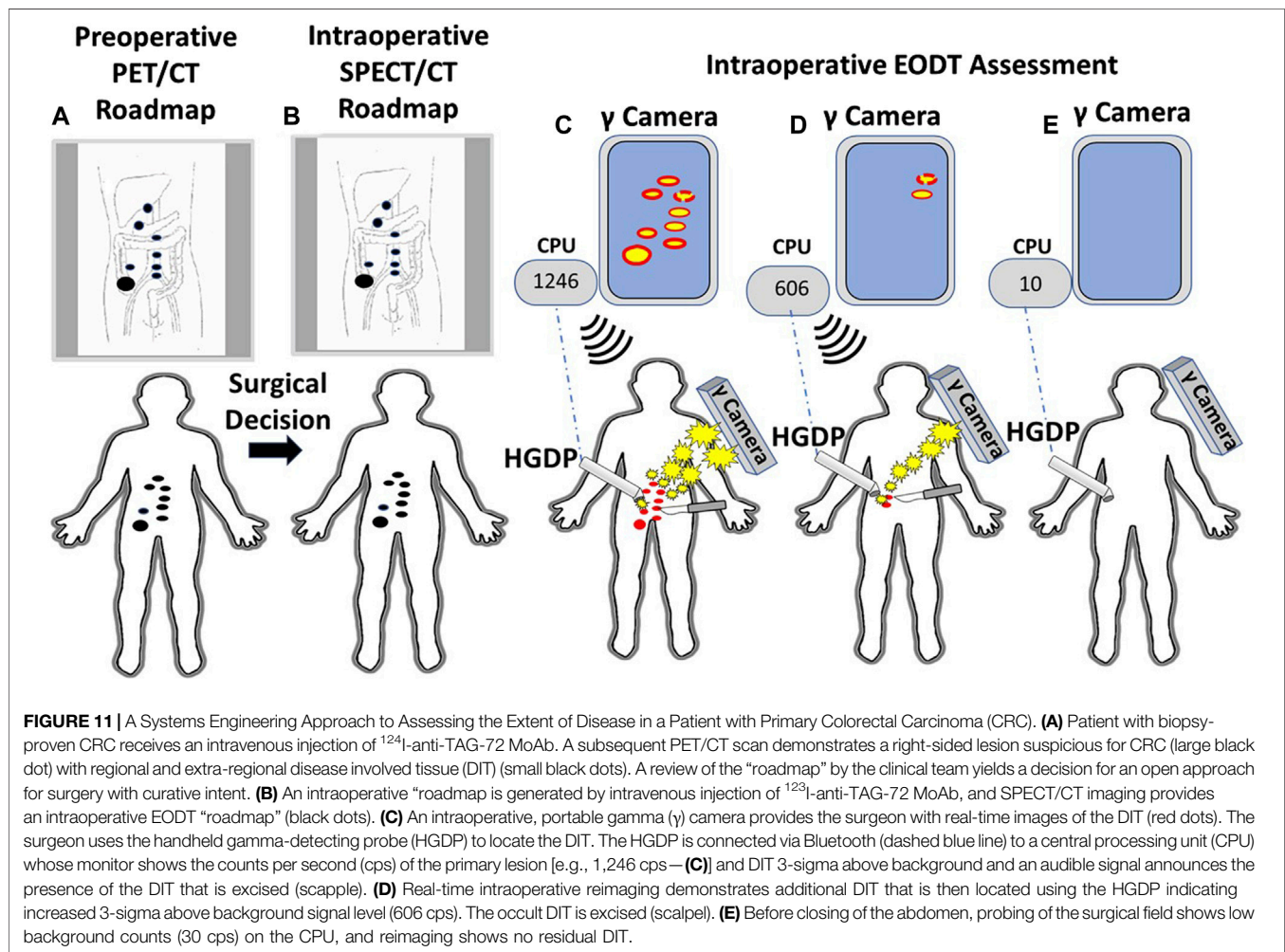


95 of 212 (45%) cases with unresectable, grossly evident HGDP (+) disease involved tissue remaining at closing, followed by occult HGDP (+) DIT in another 43/212 (20%) of the cases. We see again a subgroup where there is a significant ($p = <0.0001$) survival advantage following the removal of all HGDP (+) tissue. Whereas most studies focus on short-term 5-year survival, Panel C represents a minimum of 15-year survival data from 92 primary CRC patients who underwent ADCS following ¹²⁵I-CC49 injection [42]. It is important to note that pStage was a significant prognostic variable at each 5-year interval. Although routine pathology is not the best gold standard to judge the impact of EODT assessment, its clinical importance is critical.

Thirdly, in the case of recurrent CRC (Figures 10A, B), as with primary CRC, TAG-72ADCS can provide a significant survival advantage to a distinct group of patients. Panel A indicates that we took all comers for our clinical studies [119]. At least 40% (53/131 patients) enrolled were unresectable by ADCS but were addressed by traditional surgery. Another 29 (22%) of patients were found to be unresectable and had HGDP (+) tissue remaining at closing. For the group of 49 patients (37%), there was a significant survival advantage ($p < 0.0001$) as compared to the group of

unresectable cases. Panel B depicts the 5-year survival of the 212 primary and recurrent CRC patients who underwent ADCS with either B72.3, CC49, or CC83 mMoAbs over 14 years [38]. Again, we see three distinct populations. The poorest survival is associated with 95 of 212 (45%) cases with unresectable, grossly evident HGDP (+) disease involved tissue remaining at closing, followed by occult HGDP (+) DIT in another 43/212 (20%) of the cases. We see again a subgroup where there is a significant ($p = <0.0001$) survival advantage following the removal of all HGDP (+) tissue. Whereas most studies focus on short-term 5-year survival, Panel C represents a minimum of 15-year survival data from 92 primary CRC patients who underwent ADCS following ¹²⁵I-CC49 injection [40]. It is important to note that pStage was a significant prognostic variable at each 5-year interval. Although routine pathology is not the best gold standard to judge the impact of EODT assessment, its clinical importance is critical.

Is there a future for our technology? The answer is yes! The future operating room (OR) goals are to provide the surgeon with real-time information designed to enhance the surgical team's precision, improving patient safety and survival. These changes will improve OR efficiency, leading to more cost-effective solid tumor surgery. A literature search of PubMed



for articles written in English from 1984, the year of our first clinical case report results [135] to 2024, —using Medical Subject Heading: image-guided paired with secondary terms including surgery, imaging, fluorescence, and molecular, as well as cancer biomarkers, and gamma camera and probe—showed a plethora of publications, most of which written in the last 10 years, demonstrating continued progress in the development of the technologies critical to our concept.

Our concept of molecular imaging integrates with the technologies associated with computer-assisted minimally invasive surgery (aka, robotic surgery) and image-guided surgery. As such, intraoperative CT and MRI images only provide real-time anatomic data. However, adding intraoperative nuclear molecular imaging using a portable gamma camera will provide location information based on tumor biology independent of tissue location. Fluorescence-guided surgery can be critical for real-time intraoperative assessment of resection margins and superficial occult tumors. Studies are ongoing to look at the ability of dual-labeled preferential locators to assess EODT at the margins and metastatic sites. The next-generation of Bluetooth-

enabled gamma probes and fluorescence probes/gamma cameras for intraoperative detection of DIT are under development for both invasive and minimally invasive cancer surgery. Integration of the resulting intraoperative data and its real-time display to the surgeon will require information-bearing monitors throughout the OR. In addition, the surgeon will have a heads-up display that permits viewing of the images and other data without looking up at one of the monitors [136, 137]. Ultimately, the surgeon’s capability to make real-time clinical decisions leads to complete resection of all DIT while reducing the cost of care and improving patient outcomes.

DATA AVAILABILITY STATEMENT

The datasets presented in this article are not readily available because the data sets dealing with RIGS research are up to 30 years old and no longer are available in any form. The data from the gastrinoma patients is available upon request. Requests to access the datasets should be directed to emerituschuck@gmail.com.

AUTHOR CONTRIBUTIONS

Although the article was written by CH, each of the authors were involved in the conceptualization and the editing of the manuscript and its figures and tables. CM and EM conducted the clinical studies reported in this study. All authors contributed to the article and approved the submitted version.

FUNDING

The author(s) declare that financial support was received for the research, authorship, and/or publication of this article. Funding for the prior clinical studies presented in this current manuscript was previously provided by grants from the NIH, as well as from Neoprobe Corporation (now Navidea Biopharmaceuticals, Inc.). No research funds supported the

study design, collection, analysis, interpretation of data, the writing of this article or the decision to submit it for publication.

CONFLICT OF INTEREST

Authors CH, GC, CM, JM, and EM were employed by Actis Medical, LLC.

ACKNOWLEDGMENTS

The authors want to thank Richard A. Hoefer, D.O., F.A.C.S. for his detailed review and insightful suggestions and edits of the manuscript. The authors also thank Stephen P. Povoski M.D. for his continued support and timely suggestions in this endeavor.

REFERENCES

- Hall NC, Ruutinen AT. Colorectal Cancer. *Surg Oncol Clin North America* (2018) 27:289–302. doi:10.1016/j.soc.2017.11.004
- Albandar MH, Cho MS, Bae SU, Kim NK. Surgical Management of Extra-regional Lymph Node Metastasis in Colorectal Cancer. *Expert Rev Anticancer Ther* (2016) 16:503–13. doi:10.1586/14737140.2016.1162718
- Guraya SY. Pattern, Stage, and Time of Recurrent Colorectal Cancer after Curative Surgery. *Clin Colorectal Cancer* (2019) 18:e223–e228. doi:10.1016/j.clcc.2019.01.003
- Gately L, Jalali A, Semira C, Faragher I, Croxford M, Ananda S, et al. Stage Dependent Recurrence Patterns and post-Recurrence Outcomes in Non-metastatic colon Cancer. *Acta Oncologica* (2021) 60:1106–13. doi:10.1080/0284186X.2021.1943519
- Saha S, Johnston G, Korant A, Shaik M, Kanaan M, Johnston R, et al. Aberrant Drainage of sentinel Lymph Nodes in colon Cancer and its Impact on Staging and Extent of Operation. *Am J Surg* (2013) 205:302–6. doi:10.1016/j.amjsurg.2012.10.029
- Boekstijn I, van Oosterom MN, Dell'Oglio P, van Velden FHP, Pool M, Maurer T, et al. The Current Status and Future Prospects for Molecular Imaging-Guided Precision Surgery. *Cancer Imaging* (2022) 22:48. doi:10.1186/s40644-022-00482-2
- Schillaci O, Scimeca M, Toschi N, Bonfiglio R, Urbano N, Bonanno E. Combining Diagnostic Imaging and Pathology for Improving Diagnosis and Prognosis of Cancer. *Contrast Media Mol Imaging* (2019) 2019:9429761–10. doi:10.1155/2019/9429761
- Tiernan JP, Perry SL, Verghese ET, West NP, Yeluri S, Jayne DG, et al. Carcinoembryonic Antigen Is the Preferred Biomarker for *In Vivo* Colorectal Cancer Targeting. *Br J Cancer* (2013) 108(3):662–7. doi:10.1038/bjc.2012.605
- Voskuil FJ, Vonk J, van der Vegt B, Kruijff S, Ntziachristos V, van der Zaag PJ, et al. Intraoperative Imaging in Pathology-Assisted Surgery. *Nat Biomed Eng* (2021) 6:503–14. doi:10.1038/s41551-021-00808-8
- Hall NC, Nichols SD, Povoski SP, James IA, Wright CL, Harris R, et al. Intraoperative Use of a Portable Large Field of View Gamma Camera and Handheld Gamma Detection Probe for Radioguided Localization and Prediction of Complete Surgical Resection of Gastrinoma: Proof of Concept. *J Am Coll Surgeons* (2015) 221:300–8. doi:10.1016/j.jamcollsurg.2015.03.047
- Lauwerends LJ, Abbasi H, Bakker Schut TC, Van Driel PBAA, Hardillo JAU, Santos IP, et al. The Complementary Value of Intraoperative Fluorescence Imaging and Raman Spectroscopy for Cancer Surgery: Combining the Incompatibles. *Eur J Nucl Med Mol Imaging* (2022) 49:2364–76. doi:10.1007/s00259-022-05705-z
- Ding H, Carlton MM, Povoski SP, Milum K, Kumar K, Kothandaraman S, et al. Site Specific Discrete PEGylation of (124)I-Labeled mCC49 Fab' Fragments Improves Tumor MicroPET/CT Imaging in Mice. *Bioconjug Chem* (2013) 24:1945–54. doi:10.1021/bc400375f
- Cutler CS, Chanda N, Shukla R, Sisay N, Cantorias M, Zambre A, et al. Nanoparticles and Phage Display Selected Peptides for Imaging and Therapy of Cancer. *Recent Results Cancer Research Fortschritte der Krebsforschung Progres Dans Les Recherches sur le Cancer* (2013) 194:133–47. doi:10.1007/978-3-642-27994-2_8
- Hitchcock CL, Povoski SP, Mojzisek CM, Martin EW, Jr. Survival Advantage Following TAG-72 Antigen-Directed Cancer Surgery in Patients with Colorectal Carcinoma: Proposed Mechanisms of Action. *Front Oncol* (2021) 11:731350. doi:10.3389/fonc.2021.731350
- Nasseri Y, Langenfeld SJ. Imaging for Colorectal Cancer. *Surg Clin North America* (2017) 97:503–13. doi:10.1016/j.suc.2017.01.002
- Benson AB, Venook AP, Al-Hawary MM, Arain MA, Chen YJ, Ciombor KK, et al. Colon Cancer, Version 2.2021, NCCN Clinical Practice Guidelines in Oncology. *J Natl Compr Cancer Netw* (2021) 19:329–59. doi:10.6004/jnccn.2021.0012
- Korngold EK, Moreno C, Kim DH, Fowler KJ, Cash BD, Chang KJ, et al. ACR Appropriateness Criteria® Staging of Colorectal Cancer: 2021 Update. *J Am Coll Radiol* (2022) 19:S208–S222. doi:10.1016/j.jacr.2022.02.012
- Iannicelli E, Di Renzo S, Ferri M, Pillozzi E, Di Girolamo M, Saporì A, et al. Accuracy of High-Resolution MRI with Lumen Distention in Rectal Cancer Staging and Circumferential Margin Involvement Prediction. *Korean J Radiol* (2014) 15:37–44. doi:10.3348/kjr.2014.15.1.37
- Fernandez LM, Parlade AJ, Wasser EJ, Dasilva G, de Azevedo RU, Ortega CD, et al. How Reliable Is CT Scan in Staging Right Colon Cancer? *Dis Colon Rectum* (2019) 62:960–4. doi:10.1097/DCR.0000000000001387
- Hong EK, Chalabi M, Landolfi F, Castagnoli F, Park SJ, Sikorska K, et al. Colon Cancer CT Staging According to Mismatch Repair Status: Comparison and Suggestion of Imaging Features for High-Risk colon Cancer. *Eur J Cancer* (2022) 174:165–75. doi:10.1016/j.ejca.2022.06.060
- Olsen ASF, Gundestrup AK, Kleif J, Thanon T, Bertelsen CA. Accuracy of Preoperative Staging with Multidetector Computed Tomography in colon Cancer. *Colorectal Dis* (2021) 23:680–8. doi:10.1111/codi.15415
- Realì C, Bocca G, Lindsey I, Jones O, Cunningham C, Guy R, et al. Influence of Incorrect Staging of Colorectal Carcinoma on Oncological Outcome: Are We Playing Safely? *Updates Surg* (2022) 74:591–7. doi:10.1007/s13304-021-01095-3
- Yukimoto R, Uemura M, Tsuboyama T, Sekido Y, Hata T, Ogino T, et al. Efficacy of PET/CT in Diagnosis of Regional Lymph Node Metastases in Patients with Colorectal Cancer: Retrospective Cohort Study. *BJS Open* (2022) 6:zrac090. doi:10.1093/bjsopen/zrac090
- Andreola S, Leo E, Belli F, Bufalino R, Tomasic G, Lavarino C, et al. Manual Dissection of Adenocarcinoma of the Lower Third of the Rectum Specimens for Detection of Lymph Node Metastases Smaller Than 5 Mm. *Cancer*. (1996) 77: 607–12. doi:10.1002/(sici)1097-0142(19960215)77:4<607::aid-cnrc4>3.3.co;2-0
- Herrera L, Villarreal JR. Incidence of Metastases from Rectal Adenocarcinoma in Small Lymph Nodes Detected by a Clearing Technique. *Dis Colon Rectum* (1992) 35:783–8. doi:10.1007/bf02050329

26. Herrera-Ornelas L, Justiniano J, Castillo N, Petrelli NJ, Stulc JP. Metastases in Small Lymph Nodes from colon Cancer. *Arch Surg* (1987) 122:1253–6. doi:10.1001/archsurg.1987.01400230039006
27. Hida J, Mori N, Kubo R, Matsuda T, Morikawa E, Kitaoka M, et al. Metastases from Carcinoma of the colon and Rectum Detected in Small Lymph Nodes by the Clearing Method. *J Am Coll Surg* (1994) 178(3):223–8.
28. Schrembs P, Martin B, Anthuber M, Schenkirsch G, Märkl B. The Prognostic Significance of Lymph Node Size in Node-Positive colon Cancer. *PLoS One* (2018) 13(8):e0201072. doi:10.1371/journal.pone.0201072
29. Bedrikovetski S, Dudi-Venkata NN, Kroon HM, Seow W, Vather R, Carneiro G, et al. Artificial Intelligence for Pre-operative Lymph Node Staging in Colorectal Cancer: A Systematic Review and Meta-Analysis. *BMC Cancer* (2021) 21(1):1058. doi:10.1186/s12885-021-08773-w
30. Hartwig M, Bräuner KB, Vogelsang R, Gögenur I. Preoperative Prediction of Lymph Node Status in Patients with Colorectal Cancer. Developing a Predictive Model Using Machine Learning. *Int J Colorectal Dis* (2022) 37:2517–24. doi:10.1007/s00384-022-04284-7
31. Rahmim A, Zaidi H. PET versus SPECT: Strengths, Limitations and Challenges. *Nucl Med Commun* (2008) 29:193–207. doi:10.1097/MNM.0b013e3282f3a515
32. Shah MH, Goldner WS, Halfdanarson TR, Bergsland E, Berlin JD, Halperin D, et al. NCCN Guidelines Insights: Neuroendocrine and Adrenal Tumors, Version 2.2018. *J Natl Compr Canc Netw* (2018) 16:693–702. doi:10.6004/jnccn.2018.0056
33. Fendler WP, Calais J, Eiber M, Flavell RR, Mishoe A, Feng FY, et al. Hope TA. Assessment of 68Ga-PSMA-11 PET Accuracy in Localizing Recurrent Prostate Cancer: A Prospective Single-Arm Clinical Trial. *JAMA Oncol* (2019) 5:856–63. doi:10.1001/jamaoncol.2019.0096
34. Kroenke M, Schweiger L, Horn T, Haller B, Schwamborn K, Wurzer A, et al. Validation of ¹⁸F-rhPSMA-7 and ¹⁸F-rhPSMA-7.3 PET Imaging Results with Histopathology from Salvage Surgery in Patients with Biochemical Recurrence of Prostate Cancer. *J Nucl Med* (2022) 63:1809–14. doi:10.2967/jnumed.121.263707
35. Rusckowski M, Gupta S, Liu G, Dou S, Hnatowich DJ. Evidence of Specificity of Radiolabeled Phage Display Peptides for the TAG-72 Antigen. *Cancer Biother Radiopharm* (2007) 22:564–72. doi:10.1089/cbr.2006.307
36. Ogunwobi OO, Mahmood F, Akingboye A. Biomarkers in Colorectal Cancer: Current Research and Future Prospects. *Int J Mol Sci* (2020) 21:5311. doi:10.3390/ijms21155311
37. Qiu L, Lin Q, Si Z, Tan H, Liu G, Zhou J, et al. A Pretargeted Imaging Strategy for EGFR-Positive Colorectal Carcinoma via Modulation of Tz-Radioligand Pharmacokinetics. *Mol Imaging Biol* (2021) 23:38–51. doi:10.1007/s11307-020-01539-z
38. Maleki F, Rezazadeh F, Varmira K. MUC1-Targeted Radiopharmaceuticals in Cancer Imaging and Therapy. *Mol Pharmaceutics* (2021) 18:1842–61. doi:10.1021/acs.molpharmaceut.0c01249
39. Kramer CS, Dimitrakopoulou-Strauss A. Immuno-Imaging (PET/SPECT)-Quo Vadis? *Molecules* (2022) 27:3354. doi:10.3390/molecules27103354
40. Martinez DA, Barbera-Guillem E, LaValle GJ, Martin EW, Jr. Radioimmunoguided Surgery for Gastrointestinal Malignancies: An Analysis of 14 Years of Clinical Experience. *Cancer Control* (1997) 4(4):505–16. doi:10.1177/107327489700400604
41. Sun D, Bloomston M, Hinkle G, Al-Saif OH, Hall NC, Povoski SP, et al. Radioimmunoguided Surgery (RIGS), PET/CT Image-Guided Surgery, and Fluorescence Image-Guided Surgery: Past, Present, and Future. *J Surg Oncol* (2007) 96:297–308. doi:10.1002/jso.20869
42. Povoski SP, Hatzaras IS, Mojzisek CM, Arnold MW, Hinkle GH, Hitchcock CL, et al. Antigen-Directed Cancer Surgery for Primary Colorectal Cancer: 15-Year Survival Analysis. *Ann Surg Oncol* (2012) 19:131–8. doi:10.1245/s10434-011-1880-3
43. Merchant J, McArthur D, Ferguson H, Ramcharan S. Concepts and Prospects of Minimally Invasive Colorectal Cancer Surgery. *Clin Radiol* (2021) 76:889–95. doi:10.1016/j.crad.2021.09.013
44. Konishi T, You YN. Complete Mesocolic Excision and Extent of Lymphadenectomy for the Treatment of Colon Cancer. *Surg Oncol Clin North America* (2022) 31:293–306. doi:10.1016/j.soc.2021.11.009
45. Pantalos G, Patsouras D, Spartalis E, Dimitroulis D, Tsourouflis G, Nikiteas N. Three-Dimensional versus Two-Dimensional Laparoscopic Surgery for Colorectal Cancer: Systematic Review and Meta-Analysis. *In Vivo* (2020) 34:11–21. doi:10.21873/invivo.11740
46. Grosek J, Ales Kosir J, Sever P, Erculj V, Tomazic A. Robotic versus Laparoscopic Surgery for Colorectal Cancer: A Case-Control Study. *Radiol Oncol* (2021) 55:433–8. doi:10.2478/raon-2021-0026
47. Tanis PJ. Minimally Invasive Surgery Improves Survival after Colorectal Cancer Resection. *Colorectal Dis* (2021) 23:2498. doi:10.1111/codi.15906
48. Wei W, Rosenkrans ZT, Liu J, Huang G, Luo QY, Cai W. ImmunoPET: Concept, Design, and Applications. *Chem Rev* (2020) 120:3787–851. doi:10.1021/acs.chemrev.9b00738
49. Long NE, Sullivan BJ, Ding H, Doll S, Ryan MA, Hitchcock CL, et al. Linker Engineering in Anti-TAG-72 Antibody Fragments Optimizes Biophysical Properties, Serum Half-Life, and High-Specificity Tumor Imaging. *J Biol Chem* (2018) 293:9030–40. doi:10.1074/jbc.RA118.002538
50. Scott AM, Akhurst T, Lee FT, Ciprotti M, Davis ID, Weickhardt AJ, et al. First Clinical Study of a Pegylated Diabody ¹²⁴I-Labeled PEG-Avp0458 in Patients with Tumor-Associated Glycoprotein 72 Positive Cancers. *Theranostics* (2020) 10:11404–15. doi:10.7150/thno.49422
51. Becker J, Schwarzenböck SM, Krause BJ. FDG PET Hybrid Imaging. *Recent Results Cancer Research Fortschritt der Krebsforschung Progres Dans Les Recherches sur le Cancer* (2020) 216:625–67. doi:10.1007/978-3-030-42618-7_19
52. Howard BA, Wong TZ. 18F-FDG-PET/CT Imaging for Gastrointestinal Malignancies. *Radiologic Clin North America* (2021) 59:737–53. doi:10.1016/j.rcl.2021.06.001
53. Brush J, Boyd K, Chappell F, Crawford F, Dozier M, Fenwick E, et al. The Value of FDG Positron Emission Tomography/computerised Tomography (PET/CT) in Pre-operative Staging of Colorectal Cancer: A Systematic Review and Economic Evaluation. *Health Technol Assess* (2011) 15:1–192. iii-iv. doi:10.3310/hta15350
54. Giesel FL, Kratochwil C, Schlittenhardt J, Dendl K, Eiber M, Staudinger F, et al. Head-to-Head Intra-individual Comparison of Biodistribution and Tumor Uptake of ⁶⁸Ga-FAPI and ¹⁸F-FDG PET/CT in Cancer Patients. *Eur J Nucl Med Mol Imaging* (2021) 48:4377–85. doi:10.1007/s00259-021-05307-1
55. Cheng Z, Wang S, Xu S, Du B, Li X, Li Y. FAPI PET/CT in Diagnostic and Treatment Management of Colorectal Cancer: Review of Current Research Status. *J Clin Med* (2023) 12:577. doi:10.3390/jcm12020577
56. Parakh S, Lee ST, Gan HK, Scott AM. Radiolabeled Antibodies for Cancer Imaging and Therapy. *Cancers (Basel)* (2022) 14:1454. doi:10.3390/cancers14061454
57. Tan N, Bavadian N, Calais J, Oyoyo U, Kim J, Turkbey IB, et al. Imaging of Prostate Specific Membrane Antigen Targeted Radiotracers for the Detection of Prostate Cancer Biochemical Recurrence after Definitive Therapy: A Systematic Review and Meta-Analysis. *J Urol* (2019) 202:231–40. doi:10.1097/JU.000000000000198
58. Thor A, Ohuchi N, Szpak CA, Johnston WW, Schlom J. Distribution of Oncofetal Antigen Tumor Associated Glycoprotein-72 Defined by Monoclonal Antibody B72.3. *Cancer Res* (1986) 46:3118–24.
59. Johnson VG, Schlom J, Paterson AJ, Bennett J, Magnani JL, Colcher D. Analysis of a Human Tumor-Associated Glycoprotein (TAG-72) Identified by Monoclonal Antibody B72.3. *Cancer Res* (1986) 46:850–7.
60. Bohdiewicz PJ. Indium-111 Satumomab Pendetide: The First FDA-Approved Monoclonal Antibody for Tumor Imaging. *J Nucl Med Technol* (1998) 26:155–71.
61. Povoski SP, Mojzisek CM, Sullivan BJ. Radioimmunoguided Surgery: Intraoperative Radioimmunodetection for the Radioguided Localization and Resection of Tumors. In: Herrmann K, Nieweg OE, Povoski SP, editors. *Radioguided Surgery: Current Applications and Innovative Directions in Clinical Practice*. Cham, Heidelberg, New York, Dordrecht, and London: Springer (2016). p. 371–417.
62. Kostakoglu L, Divgi CR, Hilton S, Cordon-Cardo C, Scott AM, Kalaigian H, et al. Preselection of Patients with High TAG-72 Antigen Expression Leads to Targeting of 94% of Known Metastatic Tumor Sites with Monoclonal Antibody I-131-CC49. *Cancer Invest* (1994) 12:551–8. doi:10.3109/07357909409023039
63. Burakir W, Schneebaum S, Kim JA, Arnold MW, Hinkle G, Berens A, et al. Pilot Study Evaluating the Intraoperative Localization of Radiolabeled Monoclonal Antibody CC83 in Patients with Metastatic Colorectal Carcinoma. *Surgery* (1995) 118:103–8. doi:10.1016/s0039-6060(05)80016-9
64. Hollandsworth HM, Nishino H, Turner M, Amirfakhri S, Filemoni F, Hoffman RM, et al. Humanized Fluorescent Tumor-Associated Glycoprotein-72 Antibody Selectively Labels Colon-Cancer Liver Metastases in Orthotopic Mouse Models. *In Vivo* (2020) 34:2303–7. doi:10.21873/invivo.12042

65. Fang L, Holford NH, Hinkle G, Cao X, Xiao JJ, Bloomston M, et al. Population Pharmacokinetics of Humanized Monoclonal Antibody HuCC49ΔCH2 and Murine Antibody CC49 in Colorectal Cancer Patients. *J Clin Pharmacol* (2007) 47:227–37. doi:10.1177/0091270006293758
66. Xiao J, Horst S, Hinkle G, Cao X, Kocak E, Fang J, et al. Pharmacokinetics and Clinical Evaluation of ¹²⁵I-Radiolabeled Humanized CC49 Monoclonal Antibody (HuCC49ΔCH₂) in Recurrent and Metastatic Colorectal Cancer Patients. *Cancer Biother Radiopharm* (2005) 20:16–26. doi:10.1089/cbr.2005.20.16
67. Zou P, Povoski SP, Hall NC, Carlton MM, Hinkle GH, Xu RX, et al. 124I-HuCC49ΔCH₂ for TAG-72 Antigen-Directed Positron Emission Tomography (PET) Imaging of LS174T colon Adenocarcinoma Tumor Implants in Xenograft Mice: Preliminary Results. *World J Surg Oncol* (2010) 8:65. doi:10.1186/1477-7819-8-65
68. Zou P, Xu S, Povoski SP, Wang A, Johnson MA, Martin EW, Jr, et al. Near-Infrared Fluorescence Labeled Anti-TAG-72 Monoclonal Antibodies for Tumor Imaging in Colorectal Cancer Xenograft Mice. *Mol Pharmaceutics* (2009) 6:428–40. doi:10.1021/mp9000052
69. Yoon SO, Lee TS, Kim SJ, Jang MH, Kang YJ, Park JH, et al. Construction, Affinity Maturation, and Biological Characterization of an Anti-tumor-associated Glycoprotein-72 Humanized Antibody. *J Biol Chem* (2006) 281:6985–92. doi:10.1074/jbc.M511165200
70. Li L, Turatti F, Crow D, Bading JR, Anderson A-L, Poku E, et al. Monodispersed DOTA-PEG-Conjugated Anti-TAG-72 Diabody Has Low Kidney Uptake and High Tumor-To-Blood Ratios Resulting in Improved ⁶⁴Cu PET. *J Nucl Med* (2010) 51:1139–46. doi:10.2967/jnumed.109.074153
71. Kuroki M, Fernsten PD, Wunderlich D, Colcher D, Simpson JF, Poole DJ, et al. Serological Mapping of the TAG-72 Tumor-Associated Antigen Using 19 Distinct Monoclonal Antibodies. *Cancer Res* (1990) 50:4872–9.
72. Gong L, Ding H, Long NE, Sullivan BJ, Martin EW, Jr, Magliery TJ, et al. A 3E8.scFv.Cys-Ir800 Conjugate Targeting TAG-72 in an Orthotopic Colorectal Cancer Model. *Mol Imaging Biol* (2018) 20:47–54. doi:10.1007/s11307-017-1096-4
73. Cohen AM, Martin EW, Jr, Lavery I, Daly J, Sardi A, Aitken D, et al. Radioimmunoguided Surgery Using Iodine 125 B72.3 in Patients with Colorectal Cancer. *Arch Surg* (1991) 126:349–52. doi:10.1001/archsurg.1991.01410270095015
74. Di Carlo V, Stella M, De Nardi P, Fazio F. Radioimmunoguided Surgery: Clinical Experience with Different Monoclonal Antibodies and Methods. *Tumori* (1995) 81(3 Suppl. 1):98–102.
75. Aftab F, Stoldt HS, Testori A, Imperatori A, Chinol M, Paganelli G, et al. Radioimmunoguided Surgery and Colorectal Cancer. *Eur J Surg Oncol (Ejso)* (1996) 22:381–8. doi:10.1016/s0748-7983(96)90352-2
76. Roselli M, Buonomo O, Piazza A, Guadagni F, Vecchione A, Brunetti E, et al. Novel Clinical Approaches in Monoclonal Antibody-Based Management in Colorectal Cancer Patients: Radioimmunoguided Surgery and Antigen Augmentation. *Semin Surg Oncol* (1998) 15:254–62. doi:10.1002/(sici)1098-2388(199812)15:4<254::aid-ssu14>3.0.co;2-v
77. Arnold M, Petty LR, Schneebaum S. The Utility of the RIGS System in Primary Colorectal Carcinoma. In: Martin JEW, editor. *Radioimmunoguided Surgery, (RIGS) in the Detection and Treatment of Colorectal Cancer*. Austin, TX: RG Landis Co (1994). p. 125–33.
78. Divgi CR, Scott AM, McDermott K, Fallone PS, Hilton S, Siler K, et al. Clinical Comparison of Radiolocalization of Two Monoclonal Antibodies (mAbs) against the TAG-72 Antigen. *Nucl Med Biol* (1994) 21:9–15. doi:10.1016/0969-8051(94)90124-4
79. Contegiacomo A, Alimandi M, Muraro R, Pizzi C, Calderopoli R, De Marchis L, et al. Expression of Epitopes of the Tumour-Associated Glycoprotein 72 and Clinicopathological Correlations in Mammary Carcinomas. *Eur J Cancer* (1994) 30:813–20. doi:10.1016/0959-8049(94)90298-4
80. Prendergast JM, Galvao da Silva AP, Eavarone DA, Ghaderi D, Zhang M, Brady D, et al. Novel Anti-sialyl-tn Monoclonal Antibodies and Antibody Drug Conjugates Demonstrate Tumor Specificity and Antitumor Activity. *MAbs* (2017) 9:615–27. doi:10.1080/19420862.2017.1290752
81. Shively JE, Beatty JD. CEA-related Antigens: Molecular Biology and Clinical Significance. *Crit Rev Oncology/Hematology* (1985) 2:355–99. doi:10.1016/s1040-8428(85)80008-1
82. Hammarstrom S, Shively JE, Paxton RJ, Beatty BG, Larsson A, Ghosh R, et al. Antigenic Sites in Carcinoembryonic Antigen. *Cancer Res* (1989) 49(17):4852–8.
83. Hammarström S. The Carcinoembryonic Antigen (CEA) Family: Structures, Suggested Functions and Expression in normal and Malignant Tissues. *Semin Cancer Biol* (1999) 9:67–81. doi:10.1006/scbi.1998.0119
84. Hong H, Sun J, Cai W. Radionuclide-Based Cancer Imaging Targeting the Carcinoembryonic Antigen. *Biomarker Insights* (2008) 3:BMI.S1124–451. doi:10.4137/bmi.s1124
85. Mayer A, Tsiompanou E, O'Malley D, Boxer GM, Bhatia J, Flynn AA, et al. Radioimmunoguided Surgery in Colorectal Cancer Using a Genetically Engineered Anti-CEA Single-Chain Fv Antibody. *Clin Cancer Res* (2000) 6:1711–9.
86. Turner MA, Lwin TM, Amirkhahri S, Nishino H, Hoffman RM, Yazaki PJ, et al. The Use of Fluorescent Anti-CEA Antibodies to Label, Resect and Treat Cancers: A Review. *Biomolecules* (2021) 11:1819. doi:10.3390/biom11121819
87. Galema HA, Meijer RPJ, Lauwerends LJ, Verhoef C, Burggraaf J, Vahrmeijer AL, et al. Fluorescence-Guided Surgery in Colorectal Cancer; A Review on Clinical Results and Future Perspectives. *Eur J Surg Oncol* (2022) 48:810–21. doi:10.1016/j.ejso.2021.10.005
88. Wong JYC, Yamauchi DM, Adhikarla V, Simpson J, Frankel PH, Fong Y, et al. First-In-Human Pilot PET Immunoimaging Study of ⁶⁴Cu-Anti-Carcinoembryonic Antigen Monoclonal Antibody (hT84.66-M5A) in Patients with Carcinoembryonic Antigen-Producing Cancers. *Cancer Biother Radiopharm* (2023) 38:26–37. doi:10.1089/cbr.2022.0028
89. Jelski W, Mroczko B. Biochemical Markers of Colorectal Cancer - Present and Future. *Cancer Manag Res* (2020) 12:4789–97. doi:10.2147/CMAR.S253369
90. Thurston MO. Development of the Gamma-Detecting Probe for Radioimmunoguided Surgery. In: Martin EW, editor. *Radioimmunoguided Surgery (RIGS) in the Detection and Treatment of Colorectal Cancer*. Austin: R.G. Landes Company (1994). p. 41–65.
91. Frangioni JV. The Problem Is Background, Not Signal. *Mol Imaging* (2009) 8:303–4.
92. Gutowski M, Framery B, Boonstra MC, Garambois V, Quenet F, Dumas K, et al. SGM-101: An Innovative Near-Infrared Dye-Antibody Conjugate that Targets CEA for Fluorescence-Guided Surgery. *Surg Oncol* (2017) 26(26):153–62. doi:10.1016/j.suronc.2017.03.002
93. Vuijk FA, Hilling DE, Mieog JSD, Vahrmeijer AL. Fluorescent-Guided Surgery for sentinel Lymph Node Detection in Gastric Cancer and Carcinoembryonic Antigen Targeted Fluorescent-Guided Surgery in Colorectal and Pancreatic Cancer. *J Surg Oncol* (2018) 118:315–23. doi:10.1002/jso.25139
94. Hollandsworth HM, Turner MA, Hoffman RM, Bouvet M. A Review of Tumor-specific Fluorescence-Guided Surgery for Colorectal Cancer. *Surg Oncol* (2021) 36:84–90. doi:10.1016/j.suronc.2020.11.018
95. Achterberg FB, Deken MM, Meijer RPJ, Mieog JSD, Burggraaf J, van de Velde CJH, et al. Clinical Translation and Implementation of Optical Imaging Agents for Precision Image-Guided Cancer Surgery. *Eur J Nucl Med Mol Imaging* (2021) 48:332–9. doi:10.1007/s00259-020-04970-0
96. Benson JR, van Leeuwen FWB, Sugie T. Editorial: State-Of-The-Art Fluorescence Image-Guided Surgery: Current and Future Developments. *Front Oncol* (2021) 11:776832. doi:10.3389/fonc.2021.776832
97. Lauwerends LJ, van Driel PBAA, Baatenburg de Jong RJ, Hardillo JAU, Koljenovic S, Puppels G, et al. Real-Time Fluorescence Imaging in Intraoperative Decision Making for Cancer Surgery. *Lancet Oncol* (2021) 22:e186–e195. doi:10.1016/S1470-2045(20)30600-8
98. Azari F, Zhang K, Kennedy GT, Chang A, Nadeem B, Delikatny EJ, et al. Precision Surgery Guided by Intraoperative Molecular Imaging. *J Nucl Med* (2022) 63:1620–7. doi:10.2967/jnumed.121.263409
99. Meijer RPJ, Neijenhuis LKA, Zeilstra AP, Roerink SF, Bhairosingh SS, Hilling DE, et al. Data-Driven Identification of Targets for Fluorescence-Guided Surgery in Non-small Cell Lung Cancer. *Mol Imaging Biol* (2023) 25:228–39. doi:10.1007/s11307-022-01791-5
100. Sarkaria IS, Martin LW, Rice DC, Blackmon SH, Slade HB, Singhal S, et al. Pafolacianine for Intraoperative Molecular Imaging of Cancer in the Lung: The ELUCIDATE Trial. *J Thorac Cardiovasc Surg* (2023) 166:e468–e478. doi:10.1016/j.jtcvs.2023.02.025
101. Sutton PA, van Dam MA, Cahill RA, Mieog S, Polom K, Vahrmeijer AL, et al. Fluorescence-Guided Surgery: Comprehensive Review. *BJS Open* (2023) 7(3):zrad049. doi:10.1093/bjsopen/zrad049

102. Mieog JSD, Achterberg FB, Zlitni A, Hutteman M, Burggraaf J, Swijnenburg RJ, et al. Fundamentals and Developments in Fluorescence-Guided Cancer Surgery. *Nat Rev Clin Oncol* (2022) 19:9–22. doi:10.1038/s41571-021-00548-3
103. Sajedi S, Sabet H, Choi HS. Intraoperative Biophotonic Imaging Systems for Image-Guided Interventions. *Nanophotonics* (2018) 8:99–116. doi:10.1515/nanoph-2018-0134
104. Lee JYK, Cho SS, Stummer W, Tanyi JL, Vahrmeijer AL, Rosenthal E, et al. Review of Clinical Trials in Intraoperative Molecular Imaging during Cancer Surgery. *J Biomed Opt* (2019) 24(Dec):1–8. doi:10.1117/1.JBO.24.12.120901
105. Nagaya T, Nakamura YA, Choyke PL, Kobayashi H. Fluorescence-Guided Surgery. *Front Oncol* (2017) 7:314. doi:10.3389/fonc.2017.00314
106. Hentzen JEK, de Jongh SJ, Hemmer PHJ, van der Plas WY, van Dam GM, Kruijff S. Molecular Fluorescence-Guided Surgery of Peritoneal Carcinomatosis of Colorectal Origin: A Narrative Review. *J Surg Oncol* (2018) 118:332–43. doi:10.1002/jso.25106
107. Tsai WK, Zettlitz KA, Tavaré R, Kobayashi N, Reiter RE, Wu AM. Dual-Modality ImmunoPET/Fluorescence Imaging of Prostate Cancer with an Anti-PSCA Cys-Minibody. *Theranostics* (2018) 8:5903–14. doi:10.7150/thno.27679
108. de Gooyer JM, Elekonawo FMK, Bos DL, van der Post RS, Pèlerin A, Framery B, et al. Multimodal CEA-Targeted Image-Guided Colorectal Cancer Surgery Using (111) In-Labeled SGM-101. *Clin Cancer Res* (2020) 26:5934–42. doi:10.1158/1078-0432.ccr-20-2255
109. Dindere ME, Tanca A, Rusu M, Liehn EA, Bucur O. Intraoperative Tumor Detection Using Pafolacianine. *Int J Mol Sci* (2022) 23:12842. doi:10.3390/ijms232112842
110. Chapman GJ, Povoski SP, Hall NC, Murrey DA, Lee R, Martin Jr EW. Comparison of Two Threshold Detection Criteria Methodologies for Determination of Probe Positivity for Intraoperative *In Situ* Identification of Presumed Abnormal 18F-FDGavid Tissue Sites during Radioguided Oncologic Surgery. *BMC Cancer* (2014) 14:667. doi:10.1186/1471-2407-14-667
111. Chapman GJ. High Energy Gamma Detection for Minimally Invasive Surgery. Columbus (OH): The Ohio State University (2017). doctoral dissertation.
112. Hellingman D, Vidal S. The Use of Intraoperative Small and Large Field of View Gamma Cameras for Radioguided Surgery. In: *Radioguided Surgery*. Switzerland: Springer International Publishing (2016). p. 35–56. doi:10.1007/978-3-319-26051-8
113. Hall NC, Plews RL, Agrawal A, Povoski SP, Wright CL, Zhang J, et al. Intraoperative Scintigraphy Using a Large Field-Of-View Portable Gamma Camera for Primary Hyperparathyroidism: Initial Experience. *Biomed Res Int* (2015) 2015:1–10. doi:10.1155/2015/930575
114. Hoogstins CE, Weixler B, Boogerd LS, Hoppener DJ, Prevoo HA, Sier CF, et al. In Search for Optimal Targets for Intraoperative Fluorescence Imaging of Peritoneal Metastasis from Colorectal Cancer. *Biomarkers in Cancer* (2017) 9:1179299X1772825. doi:10.1177/1179299X17728254
115. Manayan RC, Hart MJ, Friend WG. Radioimmunoguided Surgery for Colorectal Cancer. *Am J Surg* (1997) 173:386–9. doi:10.1016/S0002-9610(97)00070-6
116. Arnold MW, Young DC, Hitchcock CL, Schneebaum S, Martin EW, Jr. Radioimmunoguided Surgery in Primary Colorectal Carcinoma: An Intraoperative Prognostic Tool and Adjuvant to Traditional Staging. *Am J Surg* (1995) 170:315–8. doi:10.1016/s0002-9610(99)80295-5
117. Greenson JK, Isenhardt CE, Rice R, Mojzisek C, Houchens D, Martin EW, Jr. Identification of Occult Micrometastases in Pericolonic Lymph Nodes of Duke's B Colorectal Cancer Patients Using Monoclonal Antibodies against Cytokeratin and CC49. Correlation with Long-Term Survival. *Cancer* (1994) 73:563–9. doi:10.1002/1097-0142(19940201)73:3<563::aid-cnrcr2820730311>3.0.co;2-d
118. Barbera-Guillem E, Arnold MW, Nelson MB, Martin EW, Jr. First Results for Resetting the 1202 Antitumor Immune Response by Immune Corrective Surgery in colon Cancer. *Am J Surg* (1998) 1203(176):339–43. doi:10.1016/s0002-9610(98)00192-5
119. Arnold MW, Young DM, Hitchcock CL, Barberá-Guillem E, Nieroda C, Martin EW, Jr. Staging of Colorectal Cancer: Biology vs. Morphology. *Dis Colon Rectum* (1998) 41:1482–7. doi:10.1007/BF02237292
120. Brouwer NPM, Stijns RCH, Lemmens VEPP, Nagtegaal ID, Beets-Tan RGH, Fütterer JJ, et al. Clinical Lymph Node Staging in Colorectal Cancer: a Flip of the coin? *Eur J Surg Oncol* (2018) 44:1241–6. doi:10.1016/j.ejso.2018.04.008
121. Arnold MW, Hitchcock CL, Young DC, Burak WE, Jr, Bertsch DJ, Martin EW, Jr. Intra-Abdominal Patterns of Disease Dissemination in Colorectal Cancer Identified Using Radioimmunoguided Surgery. *Dis Colon Rectum* (1996) 39:509–13. doi:10.1007/BF02058702
122. Nieroda CA, Mojzisek C, Sardi A, Ferrara PJ, Hinkle G, Thurston MO, et al. Radioimmunoguided Surgery in Primary colon Cancer. *Cancer Detect Prev* (1990) 14:651–6.
123. Martin EWJ, Carey LC. Second-Look Surgery for Colorectal Cancer. The Second Time Around. *Ann Surg* (1991) 214:321–5. doi:10.1097/0000658-199109000-00014
124. Schneebaum S, Troitsa A, Avital S, Haddad R, Kashtan H, Gitstein G, et al. Identification of Lymph Node Metastases in Recurrent Colorectal Cancer. *Recent Results Cancer Research Fortschritte der Krebsforschung Progres Dans Les Recherches sur le Cancer* (2000) 157:281–92. doi:10.1007/978-3-642-57151-0_25
125. Arnold MW, Schneebaum S, Berens A, Petty L, Mojzisek C, Hinkle G, et al. Intraoperative Detection of Colorectal Cancer with Radioimmunoguided Surgery and CC49, a Second-Generation Monoclonal Antibody. *Ann Surg* (1992) 216:627–32. doi:10.1097/0000658-199212000-00003
126. Cornelius EA, West AB. False Tumor-Positive Lymph Nodes in Radioimmunodiagnosis and Radioimmunoguided Surgery: Etiologic Mechanisms. *J Surg Oncol* (1996) 63:23–35. doi:10.1002/(sici)1096-9098(199609)63:1<23::aid-jso5>3.0.co;2-s
127. Stephens AD, Punja U, Sugarbaker PH. False-Positive Lymph Nodes by Radioimmunoguided Surgery: Report of a Patient and Analysis of the Problem. *J Nucl Med* (1993) 34:804–8.
128. Sergides IG, Austin RCT, Winslet MC. Radioimmunoguided Surgery (RIGS) in the Clinical Management of Colorectal Cancer. *Colorectal Dis* (1999) 1: 310–4. doi:10.1046/j.1463-1318.1999.00096.x
129. Hitchcock CL, Sampsel J, Young DC, Martin EW, Jr, Arnold MW. Limitations with Light Microscopy in the Detection of Colorectal Cancer Cells. *Dis Colon Rectum* (1999) 42:1046–52. doi:10.1007/BF02236701
130. Güller U, Zettl A, Worni M, Langer I, Cabalzar-Wondberg D, Viehl CT, et al. Molecular Investigation of Lymph Nodes in colon Cancer Patients Using One-step Nucleic Acid Amplification (OSNA): A New Road to Better Staging? *Cancer* (2012) 118:6039–45. doi:10.1002/cncr.27667
131. Ohlsson L, Hammarström ML, Israelsson A, Näslund L, Oberg A, Lindmark G, et al. Biomarker Selection for Detection of Occult Tumour Cells in Lymph Nodes of Colorectal Cancer Patients Using Real-Time Quantitative RT-PCR. *Br J Cancer* (2006) 95:218–25. doi:10.1038/sj.bjc.6603206
132. Bernini A, Spencer M, Frizelle S, Madoff RD, Willmott LD, McCormick SR, et al. Evidence for Colorectal Cancer Micrometastases Using Reverse Transcriptase-Polymerase Chain Reaction Analysis of MUC2 in Lymph Nodes. *Cancer Detect Prev* (2000) 24:72–9.
133. Triozzi PL, Kim JA, Aldrich W, Young DC, Sampsel JW, Martin EW. Localization of Tumor-Reactive Lymph Node Lymphocytes *In Vivo* Using Radiolabeled Monoclonal Antibody. *Cancer* (1994) 73:580–9. doi:10.1002/1097-0142(19940201)73:3<580::aid-cnrcr2820730314>3.0.co;2-b
134. Cote RJ, Houchens DP, Hitchcock CL, Saad AD, Nines RG, Greenson JK, et al. Intraoperative Detection of Occult colon Cancer Micrometastases using 125I-Radiolabeled Monoclonal Antibody CC49. *Cancer* (1996) 77:613–20. doi:10.1002/(SICI)1097-0142(19960215)77:4<613::AID-CNCR5>3.0.CO;2-H
135. Aitken DR, Hinkle GH, Thurston MO, Tuttle SE, Martin DT, Olsen J, et al. A Gamma-Detecting Probe for Radioimmune Detection of CEA-Producing Tumors. Successful Experimental Use and Clinical Case Report. *Dis Colon Rectum* (1984) 27(5):279–82. doi:10.1007/BF02555625
136. Yoon JW, Chen RE, Kim EJ, Akinduro OO, Kerezoudis P, Han PK, et al. Augmented Reality for the Surgeon: Systematic Review. *The Int J Med Robotics + Comput Assist Surg : MRCAS* (2018) 14(4):e1914. doi:10.1002/rcs.1914
137. Maier-Hein L, Vedula SS, Speidel S, Navab N, Kikinis R, Park A, et al. Surgical Data Science for Next-Generation Interventions. *Nat Biomed Eng* (2017) 1: 691–6. doi:10.1038/s41551-017-0132-7

Copyright © 2024 Hitchcock, Chapman, Mojzisek, Mueller and Martin. This is an open-access article distributed under the terms of the Creative Commons Attribution License (CC BY). The use, distribution or reproduction in other forums is permitted, provided the original author(s) and the copyright owner(s) are credited and that the original publication in this journal is cited, in accordance with accepted academic practice. No use, distribution or reproduction is permitted which does not comply with these terms.

GLOSSARY

ACR	American College of Radiology
ADCS	Antigen-directed cancer surgery
CH	Constant heavy chain region of an immunoglobulin molecule
CEA	Carcinoembryonic antigen
CPS	Counts per second
CRC	Colorectal carcinoma
CT	Computerized tomography
EODT	Extent of diseased tissue
DIT	Disease involved tissue
FAP1	Fibroblast-activating protein inhibitor
FDA	Food and Drug Administration
FDG	Fluorodeoxyglucose
HAMA	Human anti-mouse antibodies
H&E	Hematoxylin and eosin
HGDP	Handheld gamma-detecting probe
IHC	Immunohistochemical
kDa	kilodaltons
MoAb	Monoclonal antibody
mMoAb	Murine monoclonal antibody
MRI	Magnetic resonance imaging
NCCN	National Comprehensive Cancer Network
PET	Positron emission tomography
PL	Preferential locator
PSMA	Prostate-specific membrane antigen
pStage	Pathologic stage
RIGS	Radioimmunoguided surgery
scFv	Single-chain fragment variable
SPECT	Single-photon emission computed tomography
TAG-72	Tumor-associated glycoprotein-72
TBR	Tumor-to-Background Ratio (Signal to Noise Ratio)
VH	Variable heavy chain of an immunoglobulin molecule
VL	Variable light chain of an immunoglobulin molecule